



# Optimal control strategies for inhibition of protein aggregation

Thomas C. T. Michaels<sup>a,1</sup>, Christoph A. Weber<sup>a,1</sup>, and L. Mahadevan<sup>a,b,c,2</sup>

<sup>a</sup>School of Engineering and Applied Sciences, Harvard University, Cambridge, MA 02138; <sup>b</sup>Department of Physics, Harvard University, Cambridge, MA 02138; and <sup>c</sup>Department of Organismic and Evolutionary Biology, Harvard University, Cambridge, MA 02138

Edited by William A. Eaton, National Institutes of Health, Bethesda, MD, and approved June 3, 2019 (received for review March 08, 2019)

Protein aggregation has been implicated in many medical disorders, including Alzheimer's and Parkinson's diseases. Potential therapeutic strategies for these diseases propose the use of drugs to inhibit specific molecular events during the aggregation process. However, viable treatment protocols require balancing the efficacy of the drug with its toxicity, while accounting for the underlying events of aggregation and inhibition at the molecular level. To address this key problem, we combine here protein aggregation kinetics and control theory to determine optimal protocols that prevent protein aggregation via specific reaction pathways. We find that the optimal inhibition of primary and fibril-dependent secondary nucleation require fundamentally different drug administration protocols. We test the efficacy of our approach on experimental data for the aggregation of the amyloid- $\beta$ (1-42) peptide of Alzheimer's disease in the model organism *Caenorhabditis elegans*. Our results pose and answer the question of the link between the molecular basis of protein aggregation and optimal strategies for inhibiting it, opening up avenues for the design of rational therapies to control pathological protein aggregation.

amyloids | optimal control | protein aggregation

Over 50 current human diseases, including Alzheimer's disease, Parkinson's disease, and type II diabetes, are intimately connected with the aggregation of precursor peptides and proteins into pathological fibrillar structures known as amyloids (1–5). However, the development of effective therapeutics to prevent protein aggregation-related diseases has been very challenging, in part, due to the complex nature of the aggregation process itself, which involves several microscopic events operating at multiple timescales (6–8).<sup>\*</sup> A promising and recent approach is the use of molecular inhibitors designed to target selectively different types of aggregate species, including the mature amyloid fibrils, or the intermediate oligomeric species, and, in this manner, interfere directly with specific microscopic steps of aggregation (9–12). Examples of such compounds include small chemical molecules, such as the anticancer drug Bexarotene (10), molecular chaperones (13, 14), antibodies, or other organic or inorganic nanoparticles (15). Just as large quantities of the aggregates are toxic, in large doses the inhibitors themselves are also toxic, suggesting the following questions: what is the optimal control strategy (dose of inhibitor and timing of its administration) for the inhibition of aggregation that arises from a balance between the degree of inhibition and the toxicity of the inhibitor? Furthermore, most importantly, how does this optimal control strategy depend on the detailed molecular pathways involved in aggregation and its inhibition?

To address these questions, we combine kinetic theory of protein aggregation (16) with control theory (17) to devise optimal treatment protocols that emerge directly from an understanding of the molecular basis of aggregation and its inhibition. To test our theory, we consider the example of the inhibition of amyloid- $\beta$ (1-42) ( $A\beta_{42}$ ) aggregation by 2 compounds, Bexarotene (10) and DesAb<sub>29–35</sub> (15), that selectively target different microscopic events of aggregation and qualitatively

confirm the theoretically predicted efficacy of the drug protocol in a model organism, *Caenorhabditis elegans*.

## Results

**Kinetic Theory of Protein Aggregation Inhibition.** The microscopic mechanisms of irreversible protein aggregation involve a number of steps (Fig. 1A), including primary nucleation, followed by fibril elongation (18). Once a critical quantity of fibrils is formed, however, aggregation is accelerated by secondary nucleation pathways, where the rate of formation of new aggregates depends on the existing aggregate population, leading to exponential growth (19–25); examples of such secondary nucleation pathways include fibril fragmentation (19) and surface-catalyzed secondary nucleation (20–25), which is active in  $A\beta_{42}$  aggregation (22). The combined action of these diverse microscopic aggregation mechanisms on the concentration  $f(t, j)$  of aggregates of size  $j$  at time  $t$  can be quantified via a master equation (SI Appendix, Eq. S4 and subsequent discussion) (14, 16):

$$\begin{aligned} \frac{df(t, j)}{dt} = & 2k_+ M_m(t)f(t, j-1) - 2k_+ M_m(t)f(t, j) \\ & + 2k_- \sum_{i=j+1}^{\infty} f(t, i) - k_-(j-1)f(t, j) \\ & + k_1 M_m(t)^{n_1} \delta_{j, n_1} + k_2 M_m(t)^{n_2} \delta_{j, n_2} \sum_{i=n_2}^{\infty} if(t, i), \end{aligned} \quad [1]$$

## Significance

A range of medical conditions, such as Alzheimer's disease, Parkinson's disease, and type II diabetes, are linked to protein aggregation. Thus, it is imperative to develop effective therapeutic strategies to combat protein aggregation. Here, we lay out a general approach for optimizing inhibition strategies based on small molecules that suppress nucleation or growth of aggregates. Our model reveals that the optimal timing of drug administration crucially depends on whether the compound inhibits primary nucleation, secondary nucleation, or the growth of aggregates. This approach could guide the rational design of therapeutic strategies to target protein aggregation diseases.

Author contributions: L.M. conceived the research and approach; T.C.T.M. and C.A.W. performed research; T.C.T.M., C.A.W., and L.M. contributed new reagents/analytic tools; T.C.T.M., C.A.W., and L.M. analyzed data; and T.C.T.M., C.A.W., and L.M. wrote the paper.

This article is a PNAS Direct Submission.

Published under the PNAS license.

<sup>1</sup>T.C.T.M. and C.A.W. contributed equally to this work.

<sup>2</sup>To whom correspondence may be addressed. Email: lmahadev@g.harvard.edu.

This article contains supporting information online at [www.pnas.org/lookup/suppl/doi:10.1073/pnas.1904090116/-DCSupplemental](http://www.pnas.org/lookup/suppl/doi:10.1073/pnas.1904090116/-DCSupplemental).

Published online June 28, 2019.

<sup>\*</sup>We note that another key step in the development of Alzheimer's disease in humans, which precedes the aggregation process, is cleavage of amyloid precursor protein (APP) (8).

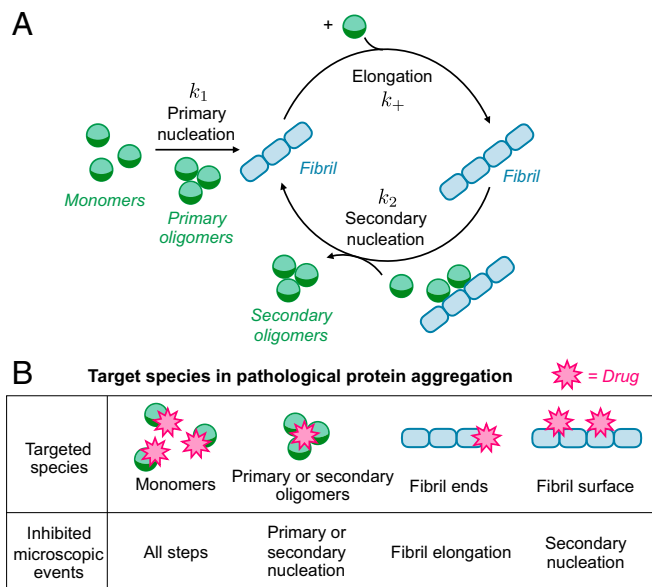


**Fig. 1.** Elementary molecular events of pathological protein aggregation and the diversity of mechanisms by which a drug can inhibit protein aggregation. (A) Fibrillar aggregates are formed through an initial primary nucleation step followed by elongation. Once a critical concentration of aggregates is reached, secondary nucleation (in the form of fragmentation or, as illustrated in the figure here, surface-catalyzed secondary nucleation) introduces a positive feedback cycle leading to exponential growth of aggregate concentration. (B) A drug can bind monomers; in addition, it can bind primary or secondary oligomers to inhibit primary or surface-catalyzed secondary nucleation. Alternatively, the drug can bind to the fibril ends or the fibril surface to suppress elongation, fragmentation or surface-catalyzed secondary nucleation.

where  $M_m(t)$  is the monomer concentration;  $k_1, k_+, k_-, k_2$  are, respectively, the rate constants for primary nucleation, elongation, fragmentation, and surface-catalyzed secondary nucleation; and  $n_1$  and  $n_2$  are the reaction orders of the primary and secondary nucleation steps. Summation of Eq. 1 over aggregate size  $j$  leads to a set of moment equations (SI Appendix, Eq. S7) for key experimental observables, including the total number concentration of aggregates  $c_a(t) = \sum_j f(t, j)$ . Solutions to such moment equations lead to a characteristic sigmoidal profile for the aggregate number concentration, with an initial lag phase followed by a saturation phase due to monomer depletion (SI Appendix, Fig. S2). During the initial lag phase, the monomer concentration is approximately constant,  $M_m(t) \approx M_m^{\text{tot}}$ , where  $M_m^{\text{tot}}$  is the total concentration of monomers. It can be shown (SI Appendix, Eq. S12) that, in this limit, the number concentration of aggregates increases exponentially with time (positive feedback),  $c_a(t) \simeq (\alpha_0/\kappa_0)e^{\kappa_0 t}$  (25), where  $\alpha_0 = k_1(M_m^{\text{tot}})^{n_1}$  is the rate of generation of new aggregates through primary nucleation and  $\kappa_0 = \sqrt{2k_+ M_m^{\text{tot}} [k_2(M_m^{\text{tot}})^{n_2} + k_-]}$  is an effective aggregate proliferation rate arising from the combined effect of aggregate growth and multiplication through the secondary nucleation pathways. In the context of inhibiting protein aggregation, a key interest is to block this positive feedback mechanism observed during the early-time exponential growth of aggregates; we will thus focus on the early stages of aggregation (rather than on the saturation phase) and assume a constant concentration for the available soluble monomers throughout. This constant-monomer concentration scenario may also be relevant in vivo, where the monomeric protein concentration is likely to be maintained at constant levels by the action of external mechanisms such as protein synthesis (26).

Protein aggregation kinetics can be inhibited in its onset or progression by the presence of a drug through 5 pathways (Fig. 1B) (14): 1) binding to free monomers, 2) binding to oligomers produced by primary nucleation (primary oligomers), 3) binding to oligomers generated by secondary nucleation (secondary oligomers), 4) binding to aggregate ends to block elongation, and 5) binding to the fibril surface to suppress fragmentation or block the production of toxic species through surface-catalyzed secondary nucleation. Since the progression of aggregation is relatively slow compared with the binding rate of drugs, an explicit treatment of the full nonlinear master equation in the presence of a drug shows that, in the limit of constant monomer concentration, the aggregate number concentration  $c_a(t)$  satisfies (see SI Appendix, section S2 for a derivation)

$$\frac{dc_a(t)}{dt} = \alpha(c_d) + \kappa(c_d) c_a(t), \quad [2a]$$

where the drug concentration  $c_d$  affects the rate parameters according to

$$\alpha(c_d) = \alpha_0 \left( \frac{1}{1 + K_m^{\text{eq}} c_d} \right)^{n_1} \left( \frac{1}{1 + K_{\text{olig},1}^{\text{eq}} c_d} \right), \quad [2b]$$

$$\kappa(c_d) = \kappa_0 \left( \frac{1}{1 + K_m^{\text{eq}} c_d} \right)^{\frac{n_2}{2}} \left( \frac{1}{1 + K_{\text{ends}}^{\text{eq}} c_d} \right)^{\frac{1}{2}} \left( \frac{1}{1 + K_{\text{surf}}^{\text{eq}} c_d} \right)^{\frac{1}{2}} \left( \frac{1}{1 + K_{\text{olig},2}^{\text{eq}} c_d} \right)^{\frac{1}{2}}. \quad [2c]$$

Note that the kinetic equation for aggregate concentration and the drug-dependent rate parameters (Eq. 2) can be explicitly derived from a microscopic description of aggregation inhibition through a nonlinear master equation describing the time evolution of the entire aggregate size distribution. They provide a link between microscopic mechanisms of aggregation and inhibition to macroscopic aggregation measurements. The complex interplay between the multiple aggregation pathways and the drug is captured explicitly by renormalized kinetic parameters  $\alpha(c_d)$  and  $\kappa(c_d)$ , which depend on the drug concentration  $c_d$  and are specific functions of the kinetic parameters of aggregation as well as the equilibrium binding constant of the drug to the targeted species,  $K_x^{\text{eq}}$ . Here,  $x$  is a placeholder for the target species and the respective pathway, i.e., monomers (m), primary or secondary oligomers (olig,1 and olig,2), fibril ends (ends), and fibril surface sites (surf). In Eq. 2, we have focused on the total aggregate particle concentration; it has, however, been shown that low molecular weight oligomers are key cytotoxic species linked to protein aggregation (27–29). To account for this situation, in SI Appendix, Eq. S15, we show that, in the constant-monomer concentration limit, a linear proportionality relationship links  $c_a(t)$  to the concentration of oligomers. Thus, after appropriate rescaling of concentration, the same Eq. 2 can be used to describe oligomeric populations as well. Throughout this paper, we thus use the generic term “aggregate” to refer to the relevant population of toxic aggregate species.

**Optimal Control of Protein Aggregation.** To find the optimal therapeutic treatment that inhibits the formation of toxic aggregate species requires a cost functional that balances aggregate toxicity against drug toxicity:

$$C = \text{Cost} [c_a(t), c_d(t)] = \int_0^T dt \mathcal{L} (c_a(t), c_d(t)), \quad [3]$$

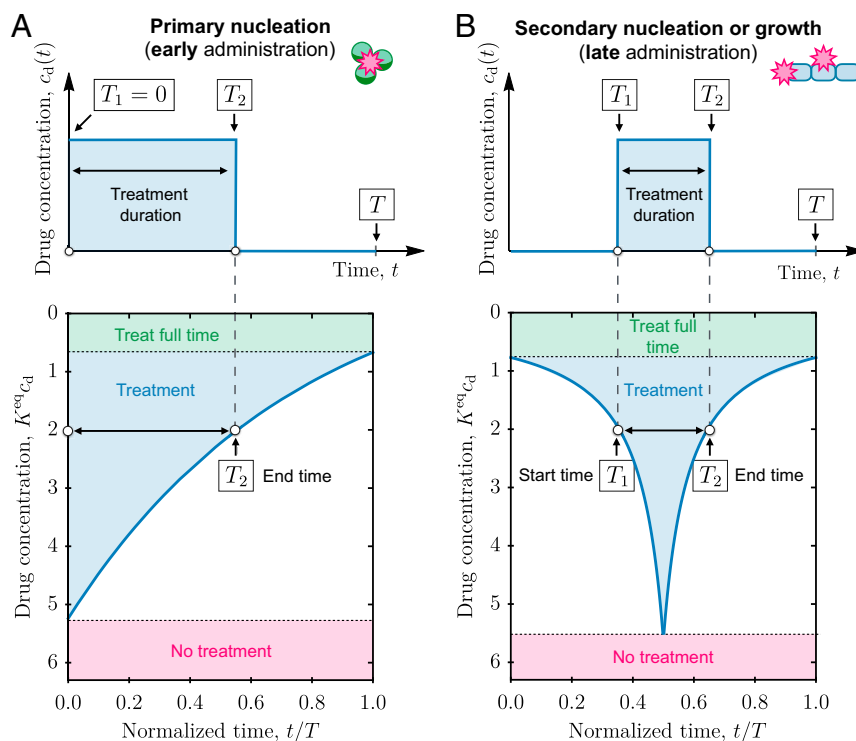


**Fig. 2.** Distinct optimal treatment protocols characterize the timing of drug administration for compounds that inhibit primary or secondary nucleation processes. (A) Optimal treatment protocol for the administration of a drug that inhibits primary nucleation (*Top*). In this case, the drug must be administered as early as possible ( $T_1 = 0$ ) and for a duration  $T_2$ . Increasing drug concentration decreases the overall duration  $T_2$  of the optimal treatment (*Bottom*) but without affecting the need for an early administration. When the drug concentration is large, no treatment is favorable (pink), while at low drug concentrations, the optimal treatment can take the full available time  $T$  (green). (B) For a drug that inhibits either fibril elongation or secondary nucleation, a late, rather than early, administration of the drug is required (*Top*). The optimal treatment protocol is thus characterized by 2 switching times,  $T_1$  and  $T_2$ , that define the start and the end of drug administration, respectively (*Bottom*). The duration of the treatment,  $T_2 - T_1$ , decreases with increasing concentration of the drug. The parameters used in the plots are:  $\zeta \kappa_0 / (\alpha_0 K_{\text{oligo},1}^{\text{eq}}) = 0.6$ ,  $\kappa_0 T = 1.3$  (A); and  $\zeta \kappa_0 / (\alpha_0 K_{\text{surf}}^{\text{eq}}) = 10$ ,  $\kappa_0 T = 4.5$  (B).

where  $T$  is the total available time for treatment, and  $\mathcal{L}$  is a function that characterizes the cost rate that increases for larger aggregate and drug concentrations.  $\mathcal{L}$  is expected to be a non-linear and monotonically increasing function of drug and aggregate concentrations. In the absence of detailed experimental insights into the form of  $\mathcal{L}$ , we linearize and use the following monotonous form of the cost function  $\mathcal{L} = c_a(t) + \zeta c_d(t)$ , where  $\zeta > 0$  quantifies the relative toxicity of aggregate and drug molecules. In *SI Appendix, section S3.7*, we show that the predictions from the linearized cost function remain qualitatively valid also in the case of a nonlinear cost function of the form  $\mathcal{L} = c_a(t)^n + \zeta c_d(t)^n$ . Future experiments may provide detailed insights into the specific form of the cost function allowing to scrutinize our prediction quantitatively. The optimal drug administration protocol  $c_d(t)$  minimizes the cost functional Eq. 3 given the aggregation dynamics governed by Eq. 2, thus enabling us to couch our problem within the realm of classical optimal control theory (17) that allows for bang-bang control solutions, given the linear nature of the cost function.

Indeed, the optimal treatment protocol consists of using piecewise constant concentration levels of the drug over varying time spans of the treatment (Fig. 2A and B) determined by the drug toxicity, the aggregation kinetic parameters, and the mechanism of inhibition (*SI Appendix, section S3*). In this protocol,  $T_1$  is the waiting time for drug administration,  $T_2 - T_1$  denotes the time period during which the drug is applied, and  $T - T_2$ , is a drug-free period after treatment. We find that, depending on whether the drug suppresses selectively primary nucleation or secondary nucleation and growth at the ends of the aggregates, the optimal

protocol for drug administration is fundamentally distinct (30).<sup>†</sup> When the drug inhibits primary nucleation ( $\alpha = \alpha(c_d)$ ,  $\kappa = \kappa_0$ ; Fig. 2A), there is no waiting period for drug administration ( $T_1 = 0$ , “early administration”), and the optimal treatment duration reads

$$T_2 = T - \frac{1}{\kappa_0} \ln \left( \frac{\zeta c_d \kappa_0}{\alpha_0 - \alpha} \right). \quad [4]$$

When the drug affects secondary nucleation or elongation ( $\kappa = \kappa(c_d)$ ,  $\alpha = \alpha_0$ ; Fig. 2B), the optimal protocol is qualitatively different: the drug must be administered after a waiting period  $T_1$  (“late administration”) and the optimal treatment duration is

$$T_2 - T_1 = \frac{\kappa_0}{\kappa_0 - \kappa} \left[ T - \frac{1}{\kappa_0} \ln \left( \frac{\zeta c_d \kappa_0^2}{\alpha_0 (\kappa_0 - \kappa)} \right) \right]. \quad [5]$$

In either case, the optimal treatment time decreases with increasing drug concentration or toxicity. Moreover, at low drug concentrations, there is a regime where the drug must be administered for the full time period  $T$ , while if the drug concentration exceeds a critical threshold,  $c_d > (\alpha_0 / \zeta \kappa_0) e^{\kappa_0 T}$ , the preferable

<sup>†</sup>Note that the distinction between “early” and “late” administration is relative to the overall, macroscopic timescale of aggregation,  $\kappa_0^{-1}$ , and available time,  $T$ ; it is thus not related to the time required for secondary nucleation to dominate over primary nucleation the production of new aggregates, which occurs very early in the lag phase (30). In fact, secondary nucleation dominates the production of new aggregates both during an early and a late administration of the drug.

choice is no treatment. The optimal treatment duration corresponds to a minimum in cost and reflects the competition between drug-induced suppression of aggregates and drug toxicity (Fig. 3A). The achievability of optimal treatment conditions is determined by the curvature of the cost function at the optimal treatment, which approximately reads  $(\kappa_0 - \kappa)\zeta c_d$  (SI Appendix, section S3.4.4). Lower curvatures around the optimal treatment parameters facilitates a robust possibility to find mostly optimal treatment conditions.

Our optimization approach allows to use the cost function to compare quantitatively different inhibition strategies and to identify the regions in the parameter space where a certain strategy is to be preferred over another; we illustrate this idea by comparing the costs for inhibition of primary or secondary nucleation (Fig. 3B and SI Appendix, section S3.4.6). We find that at large drug concentrations, and short available times  $\kappa_0 T$ , the inhibition of primary nucleation represents the optimal treatment strategy compared with the inhibition of secondary nucleation or elongation, as the former strategy exhibits lower cost. Indeed, a drug that inhibits primary nucleation must be administered from the beginning. Hence, preventing aggregation over a longer time  $\kappa_0 T$  necessarily requires longer periods of drug administration, eventually making the inhibition of primary nucleation costlier than blocking secondary nucleation at later stages. A boundary line, corresponding to equal costs for both strategies, separates the regimes of optimal treatment. The position of the boundary line depends on the relative affinity of the drug to the primary oligomers compared with secondary

oligomers, fibril ends, or fibril surfaces. Increasing drug toxicity shifts the boundary line to the right, hence favoring inhibition of primary nucleation. Another interesting parameter to consider is the initial level of aggregates, which provides a measure of preaging of the system; we find (SI Appendix, section S3.6) that increasing the initial level of aggregates shifts the boundary line to the left, hence disfavoring the inhibition of primary nucleation. Overall, for known values of the relative toxicity, our approach suggests how to select specific drugs corresponding to different mechanisms of action either in an early or late stage of the detection of protein aggregation disorders and depending on experimentally accessible parameters, such as drug affinity.

We next use the cost function to characterize longevity gain as a function of the parameters of drug-induced inhibition of aggregation (Fig. 3C and SI Appendix, section S3.4.5). We define the life time as the time at which the cost reaches a critical value corresponding to the cost that a cell or an organism can tolerate before it dies. In the absence of any drug treatment, the cost function grows exponentially with available time  $T$ , i.e.,  $\text{Cost}(c_d = 0) \simeq (\alpha_0/\kappa_0^2) e^{\kappa_0 T}$ . Crucially, the addition of a drug following the optimized treatment protocol lowers the cost down to a linear increase in time,  $\text{Cost}_{\text{opt}} \simeq \zeta c_d T$ . Hence, the difference in life times between an optimized treatment and the situation when no treatment is applied can be significant. The expected life time as a function of treatment duration displays a distinct maximum where the gain in longevity is maximal in correspondence of the optimal treatment protocol (Fig. 3D). The maximal life expectancy decreases with increasing drug concentration.

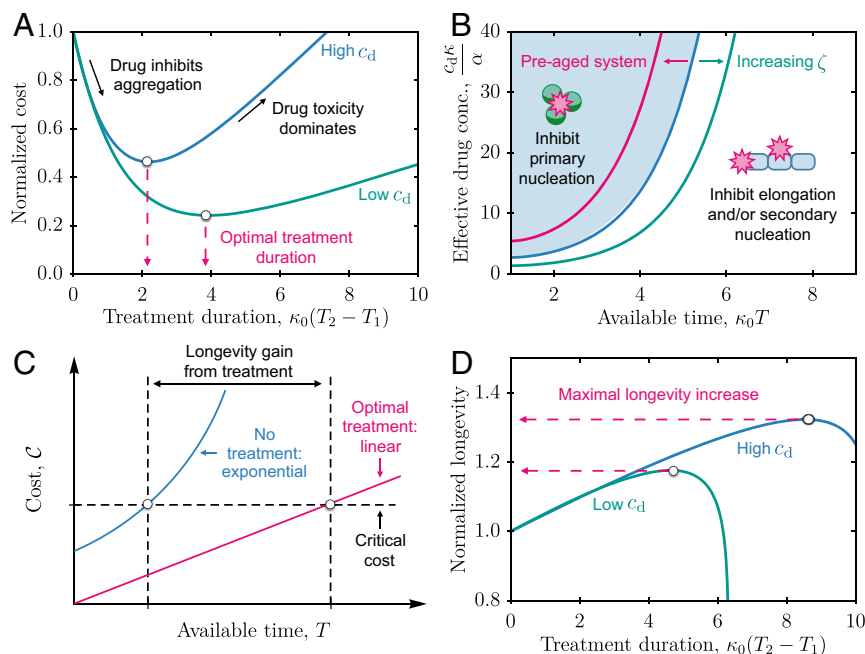


**Fig. 3.** Comparison between different inhibition strategies and predictions of lifetime gain due to optimal treatment. (A) The normalized cost,  $\text{Cost}/\text{Cost}(c_d = 0)$ , for the inhibition of secondary nucleation, has a minimum (Eq. 5) as function of the dimensionless treatment duration  $\kappa_0(T_2 - T_1)$ . At lower drug concentration (green line), the minimum of the cost becomes broader, indicating an easier access to the optimal protocol in the presence of fluctuations or limited knowledge of cellular kinetic parameters or concentrations. (B) Phase diagram indicating the region of parameter space where inhibition of primary nucleation has a lower cost than inhibition of secondary nucleation or growth. The green line indicates how the boundary line shifts when drug toxicity is increased by a factor of 2. Similarly, the pink line indicates how the boundary line shifts when the system is preaged, i.e., an increased concentration of aggregates initially. Note that  $c_d \kappa / \alpha \simeq (\kappa_0 / \alpha_0) c_d^{3/2} K_{10}^{\text{eq}} / \sqrt{K_{2nd}^{\text{eq}}}$ , where  $K_{10}^{\text{eq}}$  and  $K_{2nd}^{\text{eq}}$  are the binding constants (affinities) for the inhibition, respectively, of primary and secondary nucleation. Thus, decreasing  $K_{10}^{\text{eq}}$  or increasing  $K_{2nd}^{\text{eq}}$  favors the inhibition of secondary nucleation over primary nucleation. (C) Cost without drug (blue) and optimal cost (pink) as a function of available time  $T$ . Note the dramatic difference in the time dependence of the cost for the optimal treatment (linear in  $T$ ) and without treatment (exponential in  $T$ ). (D) Expected life expectancy as a function of treatment duration. There is a distinct maximum where the gain in life time is maximal in correspondence of the optimal treatment protocol. The parameters used in the plots are  $\alpha_0/\kappa_0 = 2 \times 10^{-8}$ ,  $\zeta = 200$ ,  $K_{\text{surf}}^{\text{eq}} = 5 \mu\text{M}^{-1}$ ,  $\kappa_0 T = 13$ ,  $c_d = 2 \mu\text{M}$  (green),  $c_d = 6 \mu\text{M}$  (blue) (A); and  $\kappa_0 \text{Cost}_c = 10^{-3.5}$  M,  $\alpha_0/\kappa_0 = 10^{-7}$ ,  $\zeta = 10$ ,  $K_{\text{surf}}^{\text{eq}} = 1 \mu\text{M}^{-1}$ ,  $c_d = 3 \mu\text{M}$  (green),  $c_d = 5 \mu\text{M}$  (blue) (D).

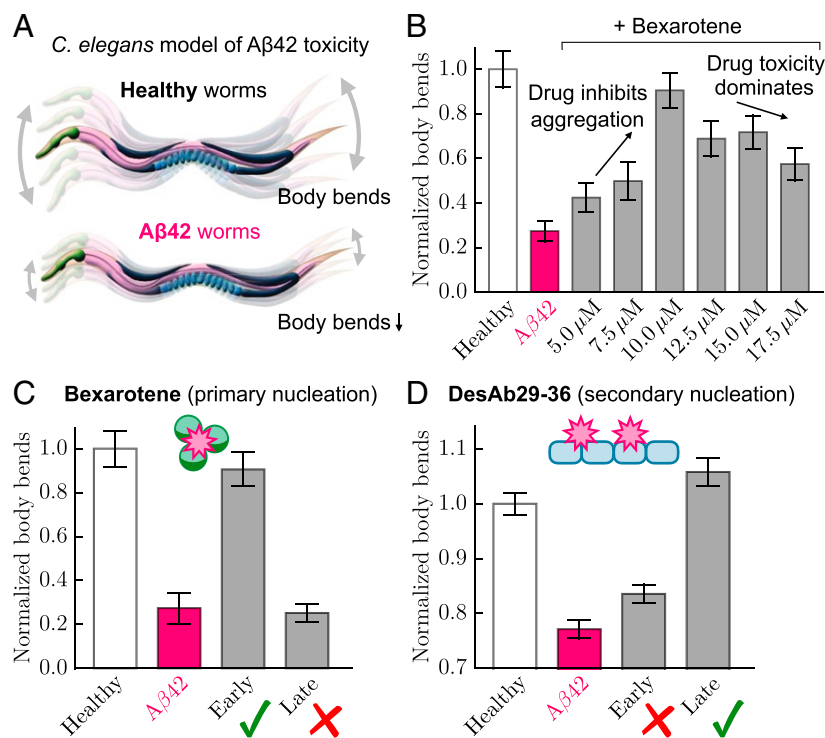


**Fig. 4.** Application to the inhibition of Alzheimer's  $A\beta_{42}$  aggregation in *C. elegans* model of  $A\beta_{42}$ -mediated toxicity. (A) Expression of  $A\beta_{42}$  in the worm's muscle cells leads to age-progressive paralysis detected through the reduction in the frequency of body bends relative to healthy worms, which do not express  $A\beta_{42}$ . (B) Low drug (Bexarotene) concentration, which selectively inhibits primary nucleation, improves worm fitness due to the inhibition of protein aggregation; however, too large drug concentrations decrease worm fitness due to toxicity of the drug (data from ref. 10). (C) Effect of early (72 h before day 0 of adulthood) and late (day 2 of adulthood) administration of Bexarotene (10  $\mu$ M) show that early administration is significantly more effective in alleviating the symptoms of worm paralysis compared with the late administration of the same drug. In the latter case, there was no observable improvement of worm fitness compared with untreated  $A\beta_{42}$  worms (data from ref. 10). (D) Effect of early (day 1 of adulthood) and late (day 6 of adulthood) administration of a selective inhibitor of secondary nucleation (DesAb<sub>29–36</sub>) (data from ref. 15) show that a late administration of DesAb<sub>29–36</sub> is more effective than an early administration in causing worm recovery. In B and C, the effect on fitness (body bends per second) was measured at day 6 of adulthood and compared with healthy worms and untreated  $A\beta_{42}$  worms, while in D, the effect on fitness was measured at day 7 of adulthood. Error bars indicate the SEM; the sample size was  $n = 200$  worms for Bexarotene experiments (10) and  $n = 500$  worms for DesAb<sub>29–36</sub> experiments (15).

**Comparison with Experiments.** We finally tested qualitatively the efficacy of the optimal protocol in practice by considering previous data (10, 15) on the inhibition of  $A\beta_{42}$  amyloid fibril formation of Alzheimer's disease using the drug Bexarotene in a *C. elegans* model of  $A\beta_{42}$ -induced dysfunction (Fig. 4A) (10, 31). Fig. 4B shows the effect of administering increasing concentrations of Bexarotene to  $A\beta_{42}$  worms in their larval stages on the frequency of body bends, a key parameter that indicates the viability of worms. At low drug concentrations, increasing Bexarotene concentration has beneficial effects on worm fitness, but too large drug concentrations decrease worm fitness. Thus, there is an optimal dose of Bexarotene (10  $\mu$ M) that leads to maximal the recovery of the worms. This optimal dose emerges from the competition between the inhibition of protein aggregation by Bexarotene (SI Appendix, Fig. S6A and B) and its toxicity (SI Appendix, Fig. S6C), as anticipated by our cost function (SI Appendix, section S3.5). At a mechanistic level, Bexarotene has been shown to affect protein aggregation by inhibiting selectively primary oligomers and hence reduce primary nucleation both in vitro (10) and in the *C. elegans* model of  $A\beta_{42}$ -induced toxicity (10) (SI Appendix, Fig. S6A). Thus, the key prediction from our model is that Bexarotene would be most effective with an early administration protocol. This prediction is in line with the experimental observations (Fig. 4C) (10) that show that the administration of Bexarotene following a late administration protocol at day 2 of worm adulthood does not induce any observable improvement in fitness relative

to untreated worms. In contrast, administering Bexarotene at the onset of the disease in the larval stages (early administration), leads to a significant recovery of worm mobility. To further support our predictions, we consider in Fig. 4D the inhibition of  $A\beta_{42}$  aggregation by another compound, DesAb<sub>29–36</sub>, which has previously been shown to inhibit selectively secondary nucleation (15). The data in this case show that DesAb<sub>29–36</sub> is more efficacious when administered at late times than during the early stages of aggregation, an observation that is in line with the theoretical predictions of our model.

## Conclusions

We have introduced a framework for estimating optimal control protocols for inhibition of irreversible protein aggregation. Overall, our results highlight and rationalize the fundamental importance of understanding the relationship between the mechanistic action, at the molecular level, of an inhibitor and the optimal timing of its administration during macroscopic profiles of protein aggregation. This understanding could have important implications in drug design against pathological protein aggregation. For example, using the cost function could provide a new platform for systematically ranking drugs in terms of their efficiency to inhibit protein aggregation measured under optimal conditions.

Our optimal protocols do not account for spatial heterogeneities, crowding, and fluctuations. Spatially dependent optimal protocols could be determined for instance by extending

our theory to reaction-diffusion systems or by including spatial organization effects, e.g., from liquid compartments (32). More generally, optimal protocols depend on the measurement accuracy of aggregate and drug concentrations and the nature and type of the cost functional. Stochasticity effects could be accounted using Kalman filter-based approaches (33). More generally, accounting explicitly in the cost function for additional factors such as organismal absorption, distribution, and clearance of the drug or its degradation over time in our theory could allow extrapolating most effective protocols from a model system, such as *C. elegans*, to clinically relevant conditions. This procedure may help to efficiently design future medical trials and would also suggest moving toward optimal drug cocktails or oscillatory protocols.

## Methods

**Determination of Optimal Protocol for Inhibition of Protein Aggregation.** To obtain the optimal inhibition protocol, we use the Pontryagin minimum principle of optimal control theory (17). In particular, the cost functional  $\text{Cost}[c_a(t), c_d(t)]$  (Eq. 3) must be minimized subject to a dynamic constraint of the form  $dc_d(t)/dt = f(c_a(t), c_d(t))$  (Eq. 2). This variational problem can be solved most conveniently by introducing a time-dependent Lagrange multiplier  $\lambda(t)$  (also known as costate variable in the context of optimal control theory) and considering the extended functional

$$\mathcal{F}[c_a(t), c_d(t)] = \text{Cost}[c_a(t), c_d(t)] + \int_0^T dt \lambda(t) \left[ \frac{dc_d(t)}{dt} - f(c_a(t), c_d(t)) \right], \quad [6]$$

where the second term ensures that the kinetic equation  $dc_d(t)/dt = f(c_a(t), c_d(t))$  is satisfied for all times  $t$ . The optimal inhibition protocol is

then determined by solving the dynamic equation  $dc_a(t)/dt = f(c_a(t), c_d(t))$  together with the Euler-Lagrange equations for  $\mathcal{F}$

$$\frac{\delta \mathcal{F}}{\delta c_a} = \frac{\partial \mathcal{L}}{\partial c_a} - \lambda(t) \frac{\partial f}{\partial c_a} - \frac{d\lambda(t)}{dt} = 0 \quad [7a]$$

$$\frac{\delta \mathcal{F}}{\delta c_d} = \frac{\partial \mathcal{L}}{\partial c_d} - \lambda(t) \frac{\partial f}{\partial c_d} = 0, \quad [7b]$$

subject to the initial condition  $c_a(0) = 0$  and the constraint  $\lambda(T) = 0$  (transversality condition). Eq. 7a describes the dynamics of the Lagrange multiplier  $\lambda(t)$ ; once  $\lambda(t)$  is known, Eq. 7b yields the optimal protocol.

Since the drug concentration is constant in the case of fast drug binding (*SI Appendix*), the optimal control consists of discrete jumps, yielding a bang-bang control of the form  $c_d = c_d^{\max} [\theta(t - T_1) - \theta(t - T_2)]$ , where  $\theta(x)$  is the Heaviside function and  $T_1$  and  $T_2$  are the switching times (Eq. 4). For the choices  $f(c_a(t), c_d(t)) = \alpha(c_d(t)) + \kappa(c_d(t))c_a(t)$  and  $\mathcal{L}(c_a(t), c_d(t)) = c_a(t) + \zeta c_d(t)$  discussed in the main text, the evolution equation for the Lagrange multiplier, Eq. 7a, reads  $d\lambda(t)/dt = -1 - \kappa(c_d(t))\lambda(t)$ , while the optimal control can be calculated from

$$\lambda(T_i) [\alpha' + \kappa' c_a(T_i)] = \zeta, \quad i = 1, 2, \quad [8]$$

where continuous derivatives with respect to  $c_d$  in Eq. 7b have been replaced by discrete jumps  $\kappa' = (\kappa_0 - \kappa(c_d^{\max}))/c_d^{\max}$  and  $\alpha' = (\alpha_0 - \alpha(c_d^{\max}))/c_d^{\max}$ . Eq. 8 determines the optimal values for the times to begin,  $T_1$ , and to end the drug treatment,  $T_2$ . Finally, considering the cases  $\alpha' = 0$  and  $\kappa' = 0$  separately, and, in the latter case, exploiting the fact that  $T_i \gg \kappa^{-1}$ , we arrive at the analytical results presented in Eqs. 4 and 5.

**ACKNOWLEDGMENTS.** We acknowledge support from the Swiss National Science Foundation (T.C.T.M.), the German Research Foundation (C.A.W.). We thank Michele Perali and Christopher M. Dobson (Center for Misfolding Diseases, University of Cambridge, Cambridge, UK) for useful discussions and for providing the extended experimental data on *C. elegans* from ref. 10.

1. T. P. J. Knowles, M. Vendruscolo, C. M. Dobson, The amyloid state and its association with protein misfolding diseases. *Nat. Rev. Mol. Cell Biol.* **15**, 384–396 (2014).
2. F. Chiti, C. M. Dobson, Protein misfolding, functional amyloid, and human disease: A summary of progress over the last decade. *Annu. Rev. Biochem.* **86**, 27–68 (2017).
3. C. M. Dobson, The amyloid phenomenon and its links with human disease. *Cold. Spring. Harb. Perspect. Biol.* **9**, a023648 (2017).
4. C. M. Dobson, Protein folding and misfolding. *Nature* **426**, 884–890 (2003).
5. D. J. Selkoe, J. Hardy, The amyloid hypothesis of Alzheimer's disease at 25 years. *EMBO Mol. Med.* **8**, 595–608 (2016).
6. J. Hardy, D. J. Selkoe, The amyloid hypothesis of Alzheimer's disease: Progress and problems on the road to therapeutics. *Science* **297**, 353–356 (2002).
7. E. Karran, J. Hardy, A critique of the drug discovery and phase 3 clinical programs targeting the amyloid hypothesis for Alzheimer disease. *Ann. Neurol.* **76**, 185–205 (2014).
8. R. J. O'Brien, P. C. Wong, Amyloid precursor protein processing and Alzheimer's disease. *Annu. Rev. Neurosci.* **34**, 185–204 (2011).
9. P. Arosio, M. Vendruscolo, C. M. Dobson, T. P. J. Knowles, Chemical kinetics for drug discovery to combat protein aggregation diseases. *Trends Pharmacol. Sci.* **35**, 127–135 (2014).
10. J. Habchi et al., An anticancer drug suppresses the primary nucleation reaction that initiates the production of the toxic A $\beta$ 42 aggregates linked with Alzheimer's disease. *Sci. Adv.* **2**, e1501244 (2016).
11. J. Habchi et al., Systematic development of small molecules to inhibit specific microscopic steps of A $\beta$ 42 aggregation in Alzheimer's disease. *Proc. Natl. Acad. Sci. U.S.A.* **114**, E200–E208 (2017).
12. S. Chia et al., SAR by kinetics for drug discovery for protein misfolding diseases. *Proc. Natl. Acad. Sci. U.S.A.* **115**, 10245–10250 (2018).
13. S. I. A. Cohen et al., A molecular chaperone breaks the catalytic cycle that generates toxic A $\beta$  oligomers. *Nat. Struct. Mol. Biol.* **22**, 207–213 (2015).
14. P. Arosio et al., Kinetic analysis reveals the diversity of microscopic mechanisms through which molecular chaperones suppress amyloid formation. *Nat. Commun.* **7**, 10948 (2016).
15. F. A. Aprile et al., Selective targeting of primary and secondary nucleation pathways in A $\beta$ 42 aggregation using a rational antibody scanning method. *Sci. Adv.* **3**, e1700488 (2017).
16. T. C. T. Michaels et al., Chemical kinetics for bridging molecular mechanisms and macroscopic measurements of amyloid fibril formation. *Annu. Rev. Phys. Chem.* **69**, 273–298 (2018).
17. L. M. Hocking, "The Pontryagin maximum principle" in *Optimal Control: An Introduction to the Theory with Applications* (Oxford University Press, Oxford, UK, 1991), pp. 85–88.
18. F. Oosawa, S. Asakura, "Kinetics of polymerization" in *Thermodynamics of the Polymerization of Protein* (Academic, London, UK, 1975), pp. 41–55.
19. T. P. J. Knowles et al., An analytical solution to the kinetics of breakable filament assembly. *Science* **326**, 1533–1537 (2009).
20. G. Ramachandran, J. B. Udgaonkar, Evidence for the existence of a secondary pathway for fibril growth during the aggregation of tau. *J. Mol. Biol.* **421**, 296–314 (2012).
21. A. M. Ruschak, A. D. Miranker, Fiber-dependent amyloid formation as catalysis of an existing reaction pathway. *Proc. Natl. Acad. Sci. U.S.A.* **104**, 12341–12346 (2007).
22. S. I. A. Cohen et al., Proliferation of amyloid- $\beta$ 42 aggregates occurs through a secondary nucleation mechanism. *Proc. Natl. Acad. Sci. U.S.A.* **110**, 9758–9763 (2013).
23. G. Meisl et al., Differences in nucleation behavior underlie the contrasting aggregation kinetics of the A $\beta$ 40 and A $\beta$ 42 peptides. *Proc. Natl. Acad. Sci. U.S.A.* **111**, 9384–9389 (2014).
24. A. Sarić et al., Physical determinants of the self-replication of protein fibrils. *Nat. Phys.* **12**, 874–880 (2016).
25. F. A. Ferrone, J. Hofrichter, W. A. Eaton, Kinetics of sickle hemoglobin polymerization. II. A double nucleation mechanism. *J. Mol. Biol.* **183**, 611–631 (1985).
26. S. I. A. Cohen et al., Nucleated polymerization with secondary pathways. I. Time evolution of the principal moments. *J. Chem. Phys.* **135**, 065105 (2011).
27. I. Benilova, E. Karran, B. De Strooper, The toxic A $\beta$  oligomer and Alzheimer's disease: An emperor in need of clothes. *Nat. Neurosci.* **15**, 349–357 (2012).
28. S. Campioni et al., A causative link between the structure of aberrant protein oligomers and their toxicity. *Nat. Chem. Biol.* **6**, 140–147 (2010).
29. G. Fusco et al., Structural basis of membrane disruption and cellular toxicity by  $\alpha$ -synuclein oligomers. *Science* **358**, 1440–1443 (2017).
30. P. Arosio, T. P. J. Knowles, S. Linse, On the lag phase in amyloid fibril formation. *Phys. Chem. Chem. Phys.* **17**, 7606–7618 (2015).
31. G. McColl et al., Utility of an improved model of amyloid-beta (A $\beta$ 1–42) toxicity in *Caenorhabditis elegans* for drug screening for Alzheimer's disease. *Mol. Neurodegener.* **7**, 57 (2012).
32. C. A. Weber, T. C. T. Michaels, L. Mahadevan, Spatial control of irreversible protein aggregation. *eLife* **8**, e4231 (2019).
33. R. F. Stengel, *Optimal Control and Estimation* (Dover Publications, 1994).

## Supplementary Information for

### Optimal control strategies for inhibition of protein aggregation

Thomas C. T. Michaels, C. A. Weber, L. Mahadevan

L Mahadevan.

E-mail: [lmahadev@g.harvard.edu](mailto:lmahadev@g.harvard.edu)

#### This PDF file includes:

Figs. S1 to S6

References for SI reference citations

## Contents

|   |           |
|---|-----------|
| <b>S1 List of symbols</b>   | <b>3</b>  |
| <b>S2 Irreversible aggregation kinetics of proteins</b>   | <b>4</b>  |
| S2.1 Kinetic equations in the absence of drug   | 4         |
| S2.1.1 Early stage of aggregation   | 6         |
| S2.1.2 Proportionality between aggregate mass and aggregate concentration   | 6         |
| S2.1.3 Proportionality between aggregate concentration and oligomer concentration   | 7         |
| S2.2 Kinetic equations in the presence of a drug affecting aggregation  | 7         |
| S2.2.1 Impact of the drug   | 7         |
| S2.2.2 Kinetic equations in the presence of a drug  | 7         |
| S2.2.3 Simplified kinetic equations in the limit of fast drug binding   | 9         |
| S2.2.4 Linearized set of equations for fast drug binding and early stage of aggregation   | 10        |
| S2.2.5 Final kinetic equation in the presence of drug and the linear relationship between particle and mass concentration of aggregates                 | 10        |
| S2.3 Kinetic equations in the presence of a drug affecting aggregation: Impact of toxic oligomers   | 10        |
| S2.3.1 Kinetic equations with oligomers in the presence of a drug   | 10        |
| S2.3.2 Simplified kinetic equations with oligomers in the limit of fast drug binding  | 11        |
| S2.3.3 Linearized set of equations for fast drug binding and early stage of aggregation with oligomers  | 12        |
| S2.3.4 Final kinetic equations with oligomers in the presence of drug and the linear relationship between particle and mass concentration of aggregates | 13        |
| <b>S3 Optimal inhibition of irreversible aggregation of proteins</b>  | <b>14</b> |
| S3.1 Introduction to variational calculus with constraint and optimal control theory  | 14        |
| S3.2 Optimal control theory applied to the inhibition of protein aggregation  | 15        |
| S3.3 Drug protocols for optimal inhibition  | 16        |
| S3.4 Optimal inhibition   | 16        |
| S3.4.1 Solutions for Lagrange multiplier (co-state variable) and solution to aggregation kinetics   | 16        |
| S3.4.2 Optimal start and end of drug treatment  | 18        |
| S3.4.3 Optimal costs and treatments deviating from the optimum  | 19        |
| S3.4.4 Sensitivity of optimal control   | 20        |
| S3.4.5 Life-time expectancy   | 20        |
| S3.4.6 Comparing strategies: Inhibition of primary nucleation against inhibition of secondary nucleation and growth at ends                             | 21        |
| S3.5 Optimal drug concentration   | 21        |
| S3.6 Optimal controls for pre-aged systems: role of initial concentration   | 21        |
| S3.6.1 Optimal control  | 21        |
| S3.6.2 Comparison between inhibition of primary or secondary nucleation depending on initial aggregate concentration                                    | 22        |
| S3.7 Optimal protocols emerging from non-linear cost functions  | 25        |



## S1. List of symbols

| Parameter         | Meaning  |
|-------------------|--|
| $k_+$             | Rate constant for aggregate elongation   |
| $k_1$             | Rate constant for primary nucleation   |
| $k_-$             | Rate constant for aggregate fragmentation  |
| $k_2$             | Rate constant for surface-catalyzed secondary nucleation   |
| $n_1$             | Reaction order of primary nucleation   |
| $n_2$             | Reaction order of secondary nucleation   |
| $M_m(t)$          | Monomer concentration  |
| $M_m^{tot}$       | Total monomer concentration (conserved)  |
| $f(t, j)$         | Concentration of aggregates of size $j$  |
| $c_a(t)$          | Aggregate number concentration $c_a(t) = \sum_j f(t, j)$ (0th moment of aggregate distribution)  |
| $M_a(t)$          | Aggregate mass concentration $M_a(t) = \sum_j j f(t, j)$ (1st moment of aggregate distribution)  |
| $c_d(t)$          | Drug concentration   |
| $K_{\times}^{eq}$ | Binding constant of drug to $\times$ = monomers (m), aggregate ends (ends), fibril surface (surf), primary or secondary oligomers (oligo,1 and oligo,2)                      |
| $\kappa_0$        | Effective rate of aggregate proliferation through aggregate elongation and secondary nucleation pathways<br>$\kappa_0 = \sqrt{2k_+ M_m^{tot} [k_2 (M_m^{tot})^{n_2} + k_-]}$ |
| $\alpha_0$        | Rate of generation of new aggregates through primary nucleation, $\alpha_0 = k_1 [M_m^{tot}]^{n_1}$  |
| $\zeta$           | Relative toxicity  |
| $T$               | Terminal time  |
| $T_1, T_2$        | Switching times (start and end of drug treatment).   |

## S2. Irreversible aggregation kinetics of proteins

In this section we show that the following single linear equation can accurately capture the early stages of irreversible protein aggregation kinetics for the aggregate number concentration (a) or the concentration of intermediate-sized oligomers (o), in the absence and even presence of a drug  $c_d$ :

$$\frac{dc_i(t)}{dt} = \alpha(c_d) + \kappa(c_d) c_i(t), \quad [S1]$$

where  $c_i$  denotes the concentration of aggregates or oligomers,  $i = a, o$ . The drug affects the aggregation process via the coefficients  $\alpha(c_d)$  and  $\kappa(c_d)$ . Below we explain the underlying approximations and present the derivation in the absence of drug (section S2.1), in the presence of drug (section S2.2) and for the case with drug and additional oligomers (section S2.3).

**S2.1. Kinetic equations in the absence of drug.** The aggregation kinetics of a system of monomers irreversibly growing into aggregates can be captured by the concentration of monomer mass  $M_m(t)$ , and the particle and mass concentrations of the aggregates/fibrils/polymers, denoted as  $c_a(t)$  and  $M_a(t)$ , respectively (1–5). The number and mass concentrations of aggregates can be defined in terms of the concentrations  $f(t, j)$  of fibrils of size  $j$  as:

$$c_a(t) = \sum_{j=n_1}^{\infty} f(t, j), \quad M_a(t) = \sum_{j=n_1}^{\infty} j f(t, j), \quad [S2]$$

where  $n_1$  denotes the size of the smallest stable aggregate (see below). These correspond to the lowest two principal moments of the aggregate size distribution, defined in general as:

$$I_n(t) = \sum_{j=n_1}^{\infty} j^n f(t, j). \quad [S3]$$

The dynamic equations for  $c_a(t)$  and  $M_a(t)$  can be obtained explicitly from considering the time evolution of the concentrations  $f(t, j)$  of aggregates of size  $j$ , which is described by the following master equation (1–5):

$$\begin{aligned} \frac{df(t, j)}{dt} &= 2k_+ M_m(t) f(t, j-1) - 2k_+ M_m(t) f(t, j) \\ &+ 2k_- \sum_{i=j+1}^{\infty} f(t, i) - k_-(j-1) f(t, j) \\ &+ k_1 M_m(t)^{n_1} \delta_{j, n_1} + k_2 M_m(t)^{n_2} \delta_{j, n_2} \sum_{i=n_2}^{\infty} i f(t, i), \end{aligned} \quad [S4]$$

$$\frac{dM_m(t)}{dt} = - \sum_{j=n_1}^{\infty} j \frac{df(t, j)}{dt}, \quad [S5]$$

where  $k_+$ ,  $k_-$ ,  $k_1$  and  $k_2$  denote the rate constants describing elongation of aggregates, fragmentation, primary and secondary nucleation, respectively, and  $n_1$ ,  $n_2$  are the reaction orders of the primary and secondary nucleation (Fig. S1). Summation of Eq. (S4) over  $j$  yields the following set of moment equations describing the dynamics of the particle and mass concentrations of aggregates:

$$\frac{dM_m(t)}{dt} = -2 \left[ k_+ M_m(t) - \frac{k_- n_1 (n_1 - 1)}{2} \right] c_a(t) \quad [S6a]$$

$$- n_1 k_1 M_m(t)^{n_1} - n_2 k_2 M_m(t)^{n_2} M_a(t) = - \frac{dM_a(t)}{dt},$$

$$\frac{dc_a(t)}{dt} = k_1 M_m(t)^{n_1} + k_2 M_m(t)^{n_2} M_a(t) + k_- [M_a(t) - (2n_1 - 1)c_a(t)], \quad [S6b]$$

Eq. (S7) have a straightforward physical interpretation in the case of linear aggregates/fibrils/polymers. The term in Eq. (S6a) proportional to the elongation rate  $k_+$  describe the decrease of monomer mass or the increase of aggregate mass through the addition of monomers at the ends of the aggregates. There are two ends per aggregate in the case of linear fibrils or polymers leading to the factor of two. The term proportional to  $k_- n_1 (n_1 - 1)/2$  describes the release of monomers associated with the formation of an unstable aggregate when a fibril breaks at a location that is closer than  $(n_1 - 1)$  bonds from one of its ends. Eq. (S6b) states that the number of aggregates in the system increases either due to primary nucleation of monomers with a rate  $k_1$ , or through surface-catalyzed, secondary nucleation with a rate  $k_2$ . We note that the surface of a linear aggregate (e.g. fibril or polymer) scales with its mass  $M_a(t)$ , while mass conservation causes both nucleation terms appear as sink terms in Eq. (S6a). The term  $k_- [M_a(t) - (2n_1 - 1)c_a(t)]$  describes the formation of new fibrils when a fibril breaks at a location that is at least  $(n_1 - 1)$  bonds away from either end.

Typically, the dominant sink term for the change in monomer mass concentration is the growth at the ends with a rate  $k_+$  (1–3). This is because changes in monomer mass due to nucleation events are negligible in Eq. (S6a) relative to growth

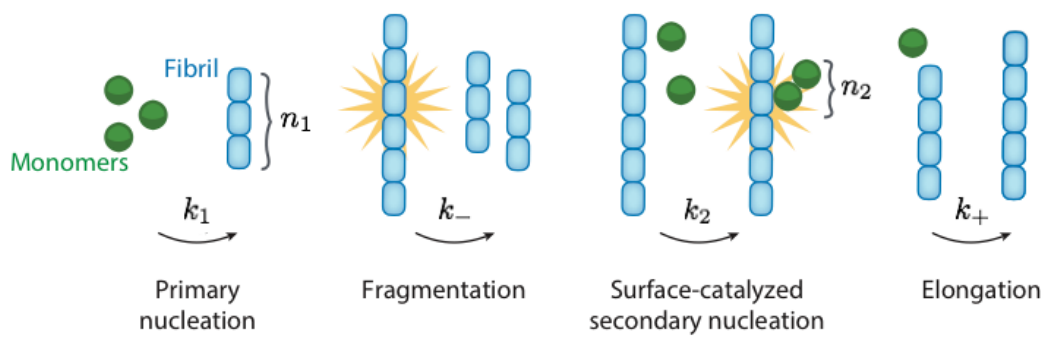


Fig. S1. Fundamental microscopic events of irreversible protein aggregation. Adapted with permission from (4).

at the ends. In particular, for most known protein aggregation processes the ratio of rates  $\nu_1 = k_1(M_m^{\text{tot}})^{n_1-2}/(2k_+) \ll 1$  and  $\nu_2 = k_2(M_m^{\text{tot}})^{n_2-1}/(2k_+) \ll 1$  (and  $\nu_2 = k_-/(2k_+M_m^{\text{tot}}) \ll 1$  for fragmentation). Indeed, the steady-state “length” of aggregates (measured in terms of the number of monomers) is given by  $\simeq 1/\sqrt{\nu_2}$  (see Supplemental Materials of Ref. (6), Section 4). Since aggregates are typically very long (several thousands of monomers), it follows  $1/\sqrt{\nu_2} \gg 1$ . Moreover, in most protein aggregating systems, such as *in vitro* assays with Alzheimer’s Amyloid- $\beta$  (7), the secondary pathway dominates primary nucleation hence  $\nu_1 \ll \nu_2 \ll 1$ . Thus we can neglect primary and secondary nucleation in the kinetic equation for the monomers, and use the conservation of monomer mass,  $dM_a/dt = -dM_m/dt$ , leading to a set of only two independent moment equations:

$$-\frac{dM_m(t)}{dt} = \frac{dM_a(t)}{dt} \simeq 2k_+ M_m(t) c_a(t), \quad [\text{S7a}]$$

$$\frac{dc_a(t)}{dt} = k_1 M_m(t)^{n_1} + [k_2 M_m(t)^{n_2} + k_-] M_a(t). \quad [\text{S7b}]$$

**S2.1.1. Early stage of aggregation.** The solution to the moment equations Eq. (S7) describes a characteristic sigmoidal profile for the aggregate number concentration: there is an initial lag phase followed by rapid growth and saturation due to monomer depletion. The initial lag phase is a direct consequence of the existence of a positive feedback mechanism in the aggregation process: as we shall see below, the couplings in Eq. (S7) between aggregate number and mass concentrations,  $c_a(t)$  and  $M_a(t)$ , lead to an exponential growth of aggregates in the early stages of aggregation, when monomers are not significantly depleted. Exponential growth slows down at the late stages of aggregation, when monomer depletion becomes important. In terms of inhibiting protein aggregation, our main interest lies in the exponential growth of aggregates. For this reason, we shall now focus our description to Eq. (S7) during the early stages of aggregation. The resulting equations are linear and are valid up to a time where the growth of aggregates deviates from an exponential growth and begins to saturate due to depletion of monomers (Fig. S2).

We consider the case where the system is initialized at  $t = 0$  with a monomer mass  $M_m(0) = M_m^{\text{tot}}$  and zero aggregates, i.e.,  $M_a(0) = 0$  and  $c_a(0) = 0$ ;  $M_m^{\text{tot}}$  refers to the total protein mass in form of aggregates and monomers in the system. During the early stages of the aggregation kinetics, the monomer mass  $M_m(t)$  hardly changes, while aggregates are already nucleated and grow. In this early stage we can thus linearize the right hand side of Eq. (S7b) by replacing the kinetic monomer mass concentration  $M_m(t)$  with the constant total protein mass  $M_m^{\text{tot}}$ . Moreover, if the change of  $M_m(t)$  is small compared  $M_m^{\text{tot}}$ , one can also replace  $M_m(t)$  with  $M_m^{\text{tot}}$  in Eq. (S7a). We thus arrive at the following simplified set of linear equations valid at the early stages of the aggregation kinetics:

$$\frac{dc_a(t)}{dt} \simeq \alpha_0 + \beta_0 M_a(t), \quad [\text{S8a}]$$

$$\frac{dM_a(t)}{dt} \simeq \mu_0 c_a(t). \quad [\text{S8b}]$$

In the equations above we abbreviated the following constant coefficients as  $\alpha_0 = k_1(M_m^{\text{tot}})^{n_1}$ ,  $\beta_0 = k_2(M_m^{\text{tot}})^{n_2} + k_-$  and  $\mu_0 = 2k_+M_m^{\text{tot}}$ . Using the initial conditions  $M_a(0) = 0$  and  $c_a(0) = 0$ , the solutions of the particle and mass concentrations of the aggregates/fibrils/polymers is

$$c_a(t) = \frac{\alpha_0 \sinh(\kappa_0 t)}{\kappa_0}, \quad [\text{S9a}]$$

$$M_a(t) = \frac{\alpha_0 [\cosh(\kappa_0 t) - 1]}{\beta_0}, \quad [\text{S9b}]$$

where the rate  $\kappa_0 = \sqrt{\mu_0 \beta_0} = \sqrt{2k_+ M_m^{\text{tot}} [k_2 (M_m^{\text{tot}})^{n_2} + k_-]}$  sets the time-scale of the exponentially growing concentrations and represents a geometrical mean of the rates characterizing the elongation and the secondary nucleation of aggregates, while primary nucleation only enters as a prefactor. This property is a consequence of restricting ourselves to the early stage of the aggregation kinetics where the two concentration fields grow exponentially. Due to their “circular” couplings this is referred to as “Hinshelwood circle” (8).

**S2.1.2. Proportionality between aggregate mass and aggregate concentration.** In the early stage of the clustering kinetics, there are two relevant time regimes,  $t \lesssim \kappa_0^{-1}$  and  $t \gtrsim \kappa_0^{-1}$ . The latter regime occurs when aggregate concentration and mass significantly varies in time. To match the initial conditions the final expression for the particle and mass concentrations of the aggregates/fibrils/polymers are written as

$$c_a(t) \simeq \frac{\alpha_0}{2\kappa_0} (e^{\kappa_0 t} - 1), \quad [\text{S10a}]$$

$$M_a(t) \simeq \frac{\alpha_0}{2\beta_0} (e^{\kappa_0 t} - 1). \quad [\text{S10b}]$$

Hence, we have a linear proportionality relationship between the two concentrations

$$M_a(t) = (\kappa_0/\beta_0) c_a(t). \quad [\text{S11}]$$

By substituting this relationship into Eq. (S8a) we obtain a single linear equation for the time evolution of the aggregate/fibril/polymer concentration,  $c_a(t)$ , in the early stage of the clustering kinetics:

$$\frac{dc_a(t)}{dt} = \alpha_0 + \kappa_0 c_a(t). \quad [S12]$$

**S2.1.3. Proportionality between aggregate concentration and oligomer concentration.** Oligomers are small aggregate species populated during amyloid formation and that have been identified as potent cytotoxins (13–16). To study their dynamics, we extend the dynamic equations Eq. (S8) to account for an additional field  $c_o(t)$  describing the concentration of oligomers. Oligomers are formed through the nucleation pathways and are depleted due to their growth into larger fibrillar structures. Thus, we have:

$$\frac{dc_o(t)}{dt} = \alpha_0 + \beta_0 M_a(t) - \mu_0 c_o(t) \quad [S13a]$$

$$\frac{dc_a(t)}{dt} = \mu_0 c_o(t). \quad [S13b]$$

Since growth is fast compared to the overall rate of aggregation  $\kappa_0$ , we can assume pre-equilibrium in Eq. (S13a). Setting  $\frac{dc_o(t)}{dt} \simeq 0$  in Eq. (S13a) yields

$$c_o(t) \simeq \frac{\alpha_0 + \beta_0 M_a(t)}{\mu_0}. \quad [S14]$$

Since  $M_a(t)$  grows exponentially with time with rate  $\kappa_0$ , also  $c_o(t)$  grows exponentially with the same rate. Thus, when  $t \gtrsim \kappa_0^{-1}$  we have a linear relationship between the aggregate concentration and the concentration of oligomers

$$c_o(t) \simeq \frac{\beta_0}{\mu_0} M_a(t) \simeq \frac{\kappa_0}{\mu_0} c_a(t). \quad [S15]$$

## S2.2. Kinetic equations in the presence of a drug affecting aggregation.

**S2.2.1. Impact of the drug.** Now we incorporate the drug into the kinetics of aggregation described by Eq. (S7). To this end, we consider three scenarios of how a drug can interfere with the aggregation kinetics (see sketch in main text, Fig. 1(a,b)):

- (i) The drug could influence the aggregation process by affecting the primary nucleation through binding to the monomers, and thereby deactivating or activating the monomers with a rate  $k_m^{\text{on}}$  or  $k_m^{\text{off}}$ , respectively. Deactivated (referred to as “bound” to the drug) monomers cannot participate in the aggregation process, i.e., they cannot nucleate to aggregates via primary and secondary nucleation, nor they can attach at the aggregate end and drive elongation.
- (ii) Moreover, the drug could suppress the secondary nucleation step of surface-catalyzed aggregation by occupying (“blocking”) the surface with a rate  $k_{\text{surf}}^{\text{on}}$  for further binding. These “blocked” aggregates (shortly referred to as “bound” to the drug) stop growing. When the drug detaches with a rate  $k_{\text{surf}}^{\text{off}}$  aggregates can again catalyze secondary nucleation events of new aggregates.
- (iii) Finally, the drug could affect the growth of the aggregates by binding (“blocking”) the two ends of the aggregates. Binding and unbinding of the drug occurs with a rate  $k_{\text{ends}}^{\text{off}}$  and  $k_{\text{ends}}^{\text{on}}$ , respectively. Aggregates with “blocked” ends, referred to as “bound” aggregates, do not grow.

All these three mechanism have been verified by *in vitro* measurement of aggregating proteins, including the aggregation of the Amyloid- $\beta$  peptide of Alzheimer’s disease (5, 9–11) or the aggregation of the protein  $\alpha$ -synuclein of Parkinson’s disease (12).

**S2.2.2. Kinetic equations in the presence of a drug.** To describe the impact of the drug we have to include additional species. In particular, we introduce species for the monomer mass concentration, and the particle and mass concentration of the aggregates/fibrils/polymers which are either active and not bound to the drug (“free”), or deactivated due to the binding of the drug (“bound”), respectively. The “bound” species do not participate in the aggregation kinetics. The kinetics of the “free” and “bound” species can be captured by the following set of equations (see Supplemental Information in Ref. (5) for a derivation from kinetic theory of irreversible aggregation):

$$\frac{dM_m^{\text{free}}(t)}{dt} \simeq -2k_+ M_m^{\text{free}}(t) c_a^{\text{free}}(t) - k_m^{\text{on}} M_m^{\text{free}}(t) c_d(t) + k_m^{\text{off}} M_m^{\text{bound}}(t), \quad [S16a]$$

$$\frac{dM_m^{\text{bound}}(t)}{dt} = k_m^{\text{on}} M_m^{\text{free}}(t) c_d(t) - k_m^{\text{off}} M_m^{\text{bound}}(t), \quad [S16b]$$

$$\frac{dM_a^{\text{free}}(t)}{dt} = 2k_+ M_m^{\text{free}}(t) c_a^{\text{free}}(t) - k_{\text{surf}}^{\text{on}} M_a^{\text{free}}(t) c_d(t) + k_{\text{surf}}^{\text{off}} M_a^{\text{bound}}(t), \quad [S16c]$$

$$\frac{dM_a^{\text{bound}}(t)}{dt} = k_{\text{surf}}^{\text{on}} M_a^{\text{free}}(t) c_d(t) - k_{\text{surf}}^{\text{off}} M_a^{\text{bound}}(t), \quad [S16d]$$

$$\frac{dc_a^{\text{free}}(t)}{dt} = k_1 M_m^{\text{free}}(t)^{n_1} + k_2 M_m^{\text{free}}(t)^{n_2} M_a^{\text{free}}(t) - k_{\text{ends}}^{\text{on}} c_a^{\text{free}}(t) c_d(t) + k_{\text{ends}}^{\text{off}} c_a^{\text{bound}}(t), \quad [S16e]$$

$$\frac{dc_a^{\text{bound}}(t)}{dt} = k_{\text{ends}}^{\text{on}} c_a^{\text{free}}(t) c_d(t) - k_{\text{ends}}^{\text{off}} c_a^{\text{bound}}(t). \quad [S16f]$$

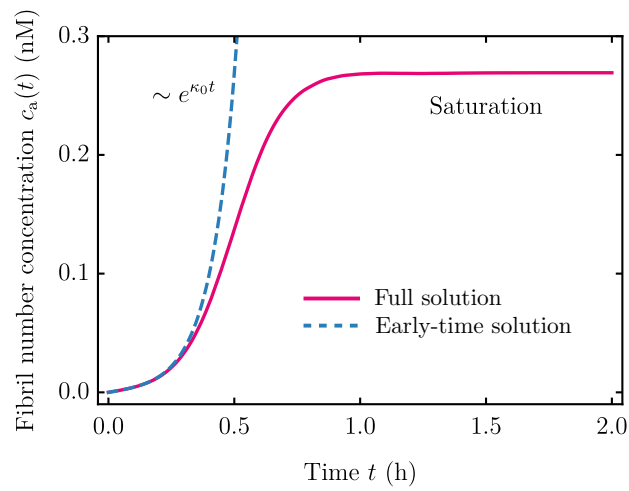


**Fig. S2.** Time course of aggregate number concentration  $c_a(t) = \sum_j f(t, j)$ , predicted by the moment equations Eq. (S7) (solid line), displays a characteristic sigmoidal profile, including an initial lag phase followed by rapid growth and saturation to a plateau due to conservation of monomer mass. The early stages of aggregation (lag-phase and rapid growth) involve exponential multiplication of aggregates with effective rate  $\kappa_0$ , as described by the early-time solution Eq. (S12) (dashed line). For drug treatments, we are interested in capturing the positive-feedback feature of aggregation associated with the initial exponential growth phase rather than in the saturation phase; for this reason we will focus our analysis on the early times of aggregation, as described by Eq. (S12). Calculation parameters are the experimentally measured aggregation rate parameters for  $A\beta_{42}$  (7):  $k_+ = 3 \times 10^6 \text{ M}^{-1}\text{s}^{-1}$ ,  $k_1 = 4 \times 10^{-4} \text{ M}^{-1}\text{s}^{-1}$ ,  $k_2 = 10^4 \text{ M}^{-2}\text{s}^{-1}$ ,  $k_- = 0$ ,  $m_{\text{tot}} = 5\mu\text{M}$ ,  $n_1 = n_2 = 2$ .

Again we have neglected the nucleation terms in the kinetic equations for the monomer mass concentration in Eq. (S16a); see section S2.1 for a discussion.

We now introduce the total monomer mass concentration  $M_m(t)$ , and the total mass and particle concentration of the aggregates,  $M_a(t)$  and  $c_a(t)$ :

$$M_m(t) = M_m^{\text{free}}(t) + M_m^{\text{bound}}(t), \quad [\text{S17a}]$$

$$M_a(t) = M_a^{\text{free}}(t) + M_a^{\text{bound}}(t), \quad [\text{S17b}]$$

$$c_a(t) = c_a^{\text{free}}(t) + c_a^{\text{bound}}(t). \quad [\text{S17c}]$$

Conservation of total protein mass (monomer and aggregates),  $M_m^{\text{tot}} = \text{constant}$ , implies

$$M_m^{\text{tot}} = M_m(t) + M_a(t) = M_m^{\text{free}}(t) + M_m^{\text{bound}}(t) + M_a^{\text{free}}(t) + M_a^{\text{bound}}(t). \quad [\text{S18}]$$

Conservation of the total amount of drug  $c_d^{\text{tot}} = \text{constant}$  gives

$$c_d^{\text{tot}} = c_d(t) + M_m^{\text{bound}}(t) + M_a^{\text{bound}}(t) + c_a^{\text{bound}}(t), \quad [\text{S19}]$$

from which the time evolution of the drug follows,

$$\frac{dc_d(t)}{dt} = -\frac{dM_m^{\text{bound}}(t)}{dt} - \frac{dM_a^{\text{bound}}(t)}{dt} - \frac{dc_a^{\text{bound}}(t)}{dt}. \quad [\text{S20}]$$

**S2.2.3. Simplified kinetic equations in the limit of fast drug binding.** Eq. (S16) can be simplified in the limit of fast binding kinetics of the drug with monomers and aggregates. Specifically, if the process of primary nucleation is slow compared to the on/off binding of the drug ( $k_1(M_m^{\text{tot}})^{n_1-1} \ll k_{\text{on}}^{\text{on}} c_d, k_{\text{off}}^{\text{off}}$ ), the time change of the bound species can be approximated as

$$\frac{dM_m^{\text{bound}}(t)}{dt} \simeq 0, \quad \frac{dc_a^{\text{bound}}(t)}{dt} \simeq 0, \quad \frac{dM_a^{\text{bound}}(t)}{dt} \simeq 0, \quad [\text{S21}]$$

leading according to Eq. (S20) to

$$\frac{dc_d(t)}{dt} \simeq 0, \quad \text{thus} \quad c_d(t) \simeq c_d, \quad [\text{S22}]$$

where  $c_d$  is the constant drug level in the system. It can be shown that any drug that is able to significantly inhibit protein aggregation must bind quickly compared to the dominant rate that contributes to the growth of aggregates. Otherwise, the effect of inhibitor does not alter significantly the aggregation reaction.

The condition Eq. (S21) further implies that there is a linear relationship between the free and bound material:

$$M_m^{\text{bound}}(t) = K_m^{\text{eq}} c_d M_m^{\text{free}}(t), \quad [\text{S23a}]$$

$$M_a^{\text{bound}}(t) = K_{\text{surf}}^{\text{eq}} c_d M_a^{\text{free}}(t), \quad [\text{S23b}]$$

$$c_a^{\text{bound}}(t) = K_{\text{ends}}^{\text{eq}} c_d c_a^{\text{free}}(t), \quad [\text{S23c}]$$

where  $K_m^{\text{eq}} = k_m^{\text{on}}/k_m^{\text{off}}$ ,  $K_{\text{surf}}^{\text{eq}} = k_{\text{surf}}^{\text{on}}/k_{\text{surf}}^{\text{off}}$  and  $K_{\text{ends}}^{\text{eq}} = k_{\text{ends}}^{\text{on}}/k_{\text{ends}}^{\text{off}}$  are the equilibrium binding constants for the drug binding to the monomers, the surface or the ends of the aggregates/fibril/polymers, respectively. These values have been accessed experimentally for various types of drugs using *in vitro* assays for protein aggregation (see (5), or Fig. 1 in Ref. (9)) or from measurements of binding kinetics using Surface Plasmon Resonance (SPR) (see Fig. 3 in Ref. (9)).

Eq. (S17) together with Eq. (S23) can be written as

$$M_m^{\text{free}}(t) = \frac{M_m(t)}{1 + K_m^{\text{eq}} c_d}, \quad [\text{S24a}]$$

$$M_a^{\text{free}}(t) = \frac{M_a(t)}{1 + K_{\text{surf}}^{\text{eq}} c_d}, \quad [\text{S24b}]$$

$$c_a^{\text{free}}(t) = \frac{c_a(t)}{1 + K_{\text{ends}}^{\text{eq}} c_d}. \quad [\text{S24c}]$$

Now we insert the relationships above into Eq. (S16a), Eq. (S16c) and Eq. (S16e), leading to three kinetic equations for the total mass of monomers  $M_m(t)$ , and the mass and particle concentration of aggregates,  $M_a(t)$  and  $c_a(t)$ , valid in the limit of fast drug binding:

$$-\frac{dM_m(t)}{dt} \simeq \frac{dM_a(t)}{dt} = 2k_+ \left( \frac{M_m(t)}{1 + K_m^{\text{eq}} c_d} \right) \left( \frac{c_a(t)}{1 + K_{\text{ends}}^{\text{eq}} c_d} \right), \quad [\text{S25a}]$$

$$\frac{dc_a(t)}{dt} = k_1 \left( \frac{M_m(t)}{1 + K_m^{\text{eq}} c_d} \right)^{n_1} + k_2 \left( \frac{M_m(t)}{1 + K_m^{\text{eq}} c_d} \right)^{n_2} \left( \frac{M_a(t)}{1 + K_{\text{surf}}^{\text{eq}} c_d} \right). \quad [\text{S25b}]$$

**S2.2.4. Linearized set of equations for fast drug binding and early stage of aggregation.** Eq. (S25) resemble the kinetic equations Eq. (S7) in the absence of drug, allowing us to further simplify Eq. (S25).

In the early regime of aggregation we can linearize the total monomer mass concentration  $M_m(t)$  around the total protein mass  $M_m^{\text{tot}}$ . Considering the initial conditions  $M_a(0) = 0$  and  $c_a(0) = 0$ , we find

$$\frac{dM_a(t)}{dt} \simeq \mu(c_d) c_a(t), \quad [\text{S26a}]$$

$$\frac{dc_a(t)}{dt} \simeq \alpha(c_d) + \beta(c_d) M_a(t), \quad [\text{S26b}]$$

where rates now depend on the drug concentration  $c_d$ :

$$\mu(c_d) = \mu_0 \left( \frac{1}{1 + K_m^{\text{eq}} c_d} \right) \left( \frac{1}{1 + K_{\text{ends}}^{\text{eq}} c_d} \right), \quad [\text{S27a}]$$

$$\alpha(c_d) = \alpha_0 \left( \frac{1}{1 + K_m^{\text{eq}} c_d} \right)^{n_1}, \quad [\text{S27b}]$$

$$\beta(c_d) = \beta_0 \left( \frac{1}{1 + K_m^{\text{eq}} c_d} \right)^{n_2} \left( \frac{1}{1 + K_{\text{surf}}^{\text{eq}} c_d} \right). \quad [\text{S27c}]$$

The constant coefficients are defined as  $\mu_0 = 2k_+ M_m^{\text{tot}}$ ,  $\alpha_0 = k_1 (M_m^{\text{tot}})^{n_1}$  and  $\beta_0 = k_2 (M_m^{\text{tot}})^{n_2}$  (see also Section S2.1.1).

**S2.2.5. Final kinetic equation in the presence of drug and the linear relationship between particle and mass concentration of aggregates.** Eq. (S26) have the form as Eq. (S8). Following the same steps as outlined in Section S2.1.2, we can derive a single kinetic equation for  $t \gtrsim \kappa(c_d)^{-1}$ , which has the characteristic rate

$$\kappa(c_d) = \sqrt{\mu(c_d)\beta(c_d)} = \kappa_0 \left( \frac{1}{1 + K_m^{\text{eq}} c_d} \right)^{(n_2+1)/2} \left( \frac{1}{1 + K_{\text{ends}}^{\text{eq}} c_d} \right)^{1/2} \left( \frac{1}{1 + K_{\text{surf}}^{\text{eq}} c_d} \right)^{1/2}, \quad [\text{S27d}]$$

and  $\kappa_0 = \sqrt{\mu_0 \beta_0} = \sqrt{2k_+ k_2 (M_m^{\text{tot}})^{n_2+1}}$ . The geometric mean arises from the exponential growth of the two concentration fields and their circular couplings and is referred to as ‘‘Hinshelwood circle’’ (8). Our final equation in the presence of the drug that is valid at the early stages of the aggregation kinetics then reads

$$\frac{dc_a(t)}{dt} = \alpha(c_d) + \kappa(c_d) c_a(t), \quad [\text{S28}]$$

where  $\kappa(c_d)$  is given in Eq. (S27d) and  $\alpha(c_d)$  is given by Eq. (S27b).

As in the absence of drug (Eq. (S12)), the aggregation kinetics with drug can be captured by a single, linear kinetic equation (Eq. (S28)) in the regime of fast drug binding and the early stage of the aggregation kinetics,  $t \gtrsim \kappa(c_d)^{-1}$ . The coefficients  $\alpha(c_d)$  and  $\kappa(c_d)$  characterize how the drug inhibits the aggregation kinetics. Most importantly, for  $c_d \rightarrow \infty$ ,  $\alpha(c_d)$  and  $\kappa(c_d)$  decrease to zero and the aggregation kinetics arrests.

**S2.3. Kinetic equations in the presence of a drug affecting aggregation: Impact of toxic oligomers.** In the following, we extend our kinetic approach to explicitly account for populations of low-molecular weight aggregates, commonly called oligomers. There is increasing recent evidence suggesting that oligomeric aggregates might carry increased cytotoxic potential compared to their high-molecular weight fibrillar counterparts (13–16). Oligomers might correspond to short fibrillar species consisting of a few to a few tens of monomers or might represent structurally distinct species from small fibrillar aggregates which thus need to undergo a conversion step before being able to recruit further monomers and grow into mature fibrils.

We thus extend the set of equations presented in the last section S2.2 by a further species, the oligomers. In addition, we allow for a further pathways of how the drug affect the aggregation kinetics. We consider the ‘‘deactivation’’ of the oligomers by blocking the surface or ends of the oligomers, thereby suppressing secondary nucleation and elongation/growth of oligomers. Since the growth and nucleation of oligomers and aggregates require monomers and because aggregates can mediate secondary nucleation of oligomers, there will be an interesting competition between oligomers and aggregates.

**S2.3.1. Kinetic equations with oligomers in the presence of a drug.** In addition to the monomer mass concentration, and the particle and mass concentration of the aggregates/fibrils/polymers we introduce a concentration of the oligomers. As in the last section, all species exists in two ‘‘states’’, i.e., they are active and not bound to the drug (‘‘free’’), or deactivated due to the binding to the drug (‘‘bound’’). The ‘‘bound’’ species no more participate in the aggregation kinetics. The kinetics of the ‘‘free’’ and ‘‘bound’’ species can be captured by the following set of equations for the monomers (m),

$$\frac{dM_m^{\text{free}}(t)}{dt} \simeq -2k_+ M_m^{\text{free}}(t) c_a^{\text{free}}(t) - k_m^{\text{on}} M_m^{\text{free}}(t) c_d(t) + k_m^{\text{off}} M_m^{\text{bound}}(t), \quad [\text{S29a}]$$

$$\frac{dM_m^{\text{bound}}(t)}{dt} = k_m^{\text{on}} M_m^{\text{free}}(t) c_d(t) - k_m^{\text{off}} M_m^{\text{bound}}(t), \quad [\text{S29b}]$$



the oligomers (o),

$$\frac{dc_o^{\text{free}}(t)}{dt} = k_1 M_m^{\text{free}}(t)^{n_1} + k_2 M_m^{\text{free}}(t)^{n_2} M_a^{\text{free}}(t) \quad [\text{S29c}]$$

$$- 2k_{\text{conv}} M_m^{\text{free}}(t)^{n_{\text{conv}}} c_o^{\text{free}}(t) - k_o^{\text{on}} c_o^{\text{free}}(t) c_d(t) + k_o^{\text{off}} c_o^{\text{bound}}(t),$$

$$\frac{dc_o^{\text{bound}}(t)}{dt} = k_o^{\text{on}} c_o^{\text{free}}(t) c_d(t) - k_o^{\text{off}} c_o^{\text{bound}}(t), \quad [\text{S29d}]$$

and the larger aggregates (a):

$$\frac{dM_a^{\text{free}}(t)}{dt} = 2k_+ M_m^{\text{free}}(t) c_a^{\text{free}}(t) - k_{\text{surf,a}}^{\text{on}} M_a^{\text{free}}(t) c_d(t) + k_{\text{surf,a}}^{\text{off}} M_a^{\text{bound}}(t), \quad [\text{S29e}]$$

$$\frac{dM_a^{\text{bound}}(t)}{dt} = k_{\text{surf,a}}^{\text{on}} M_a^{\text{free}}(t) c_d(t) - k_{\text{surf,a}}^{\text{off}} M_a^{\text{bound}}(t), \quad [\text{S29f}]$$

$$\frac{dc_a^{\text{free}}(t)}{dt} = 2k_{\text{conv}} M_m^{\text{free}}(t)^{n_{\text{conv}}} c_o^{\text{free}}(t) - k_{\text{ends,a}}^{\text{on}} c_a^{\text{free}}(t) c_d(t) + k_{\text{ends,a}}^{\text{off}} c_a^{\text{bound}}(t), \quad [\text{S29g}]$$

$$\frac{dc_a^{\text{bound}}(t)}{dt} = k_{\text{ends,a}}^{\text{on}} c_a^{\text{free}}(t) c_d(t) - k_{\text{ends,a}}^{\text{off}} c_a^{\text{bound}}(t). \quad [\text{S29h}]$$

The free oligomers are formed through primary and secondary nucleation pathways with rate constants  $k_1$  and  $k_2$ ; see Eq. (S29c). Here, the rate constants  $k_1$  and  $k_2$  describe only the formation step of oligomers and need not to correspond to the corresponding rate constants used in Sec. S2.1. As in section S2.1 we neglect the nucleation of oligomers in the kinetics of the monomer mass concentration Eq. (S29a). In addition, there is a term describing the conversion of oligomers to large aggregates with a rate  $k_{\text{conv}}$  (Eq. (S29c) and Eq. (S29g)). Large aggregates grow via their ends by recruiting free monomers with rate constant  $k_+$ ; see Eq. (S29e). The on/off kinetics between “free” and “bound” species is captured by appropriate couplings to the drug concentration  $c_d$  similar to Eq. (S16). To derive Eq. (S29a)-Eq. (S29h), we have neglected the contribution of oligomeric populations to the overall mass of aggregates; this assumption is justified as oligomers are small aggregate species that consists of maximally order 10 monomers, as opposed to mature fibrils, which typically consists of several thousands of monomeric subunits and thus are expected to dominate the aggregate mass fraction.

As in section S2.2, we introduce the total monomer mass concentration  $M_m(t)$ , and the total mass and particle concentration of the aggregates,  $M_a(t)$  and  $c_a(t)$ , as well as for mass- and particle concentration of the oligomers:

$$M_m(t) = M_m^{\text{free}}(t) + M_m^{\text{bound}}(t), \quad [\text{S30a}]$$

$$c_o(t) = c_o^{\text{free}}(t) + c_o^{\text{bound}}(t), \quad [\text{S30b}]$$

$$M_a(t) = M_a^{\text{free}}(t) + M_a^{\text{bound}}(t), \quad [\text{S30c}]$$

$$c_a(t) = c_a^{\text{free}}(t) + c_a^{\text{bound}}(t). \quad [\text{S30d}]$$

Conservation of total protein mass (monomer and aggregates),  $M_m^{\text{tot}} = \text{constant}$ , implies

$$M_m^{\text{tot}} \simeq M_m(t) + M_a(t) = M_m^{\text{free}}(t) + M_m^{\text{bound}}(t) + M_a^{\text{free}}(t) + M_a^{\text{bound}}(t). \quad [\text{S31}]$$

Note that we have neglected the mass of the oligomers in the equation above. Conservation of the total amount of drug  $c_d^{\text{tot}} = \text{constant}$  gives

$$c_d^{\text{tot}} = c_d(t) + M_m^{\text{bound}}(t) + c_o^{\text{bound}}(t) + M_a^{\text{bound}}(t) + c_a^{\text{bound}}(t) \quad [\text{S32}]$$

from which the time evolution of the drug follows,

$$\frac{dc_d(t)}{dt} = - \frac{dM_m^{\text{bound}}(t)}{dt} - \frac{dc_o^{\text{bound}}(t)}{dt} - \frac{dM_a^{\text{bound}}(t)}{dt} - \frac{dc_a^{\text{bound}}(t)}{dt}. \quad [\text{S33}]$$

**S2.3.2. Simplified kinetic equations with oligomers in the limit of fast drug binding.** Eq. (S29) can be simplified in the limit of fast binding of the drug to monomers and aggregates (for more details see section S2.2.3), such that the time change of the bound species can be approximated as

$$\frac{dM_m^{\text{bound}}(t)}{dt} \simeq 0, \quad \frac{dc_o^{\text{bound}}(t)}{dt} \simeq 0, \quad \frac{dM_a^{\text{bound}}(t)}{dt} \simeq 0, \quad \frac{dM_a^{\text{bound}}(t)}{dt} \simeq 0, \quad [\text{S34}]$$

leading according to Eq. (S33) to

$$\frac{dc_d(t)}{dt} \simeq 0, \quad \text{thus} \quad c_d(t) \simeq c_d, \quad [\text{S35}]$$

where  $c_d$  is the constant drug level in the system. The condition Eq. (S21) can also be used to equate the left hand side of Eq. (S29b), Eq. (S29d), Eq. (S29f), Eq. (S29h), to zero. This gives linear relationships between the free and bound material:

$$M_m^{\text{bound}}(t) = K_m^{\text{eq}} c_d M_m^{\text{free}}(t), \quad \text{[S36a]}$$

$$c_o^{\text{bound}}(t) = K_o^{\text{eq}} c_d c_o^{\text{free}}(t), \quad \text{[S36b]}$$

$$M_a^{\text{bound}}(t) = K_{\text{surf},a}^{\text{eq}} c_d M_a^{\text{free}}(t), \quad \text{[S36c]}$$

$$c_a^{\text{bound}}(t) = K_{\text{ends},a}^{\text{eq}} c_d c_a^{\text{free}}(t), \quad \text{[S36d]}$$

where  $K_m^{\text{eq}} = k_m^{\text{on}}/k_m^{\text{off}}$ ,  $K_o^{\text{eq}} = k_o^{\text{on}}/k_o^{\text{off}}$ ,  $K_{\text{surf},a}^{\text{eq}} = k_{\text{surf},a}^{\text{on}}/k_{\text{surf},a}^{\text{off}}$ ,  $K_{\text{ends},a}^{\text{eq}} = k_{\text{ends},a}^{\text{on}}/k_{\text{ends},a}^{\text{off}}$ , are the equilibrium binding constants for the drug binding to the monomers, the oligomers or the surface/ends of aggregates/fibril/polymers, respectively. Eq. (S30) together with Eq. (S36) can be written as

$$M_m^{\text{free}}(t) = \frac{M_m(t)}{1 + K_m^{\text{eq}} c_d}, \quad \text{[S37a]}$$

$$c_o^{\text{free}}(t) = \frac{c_o(t)}{1 + K_o^{\text{eq}} c_d}, \quad \text{[S37b]}$$

$$M_a^{\text{free}}(t) = \frac{M_a(t)}{1 + K_{\text{surf},a}^{\text{eq}} c_d}, \quad \text{[S37c]}$$

$$c_a^{\text{free}}(t) = \frac{c_a(t)}{1 + K_{\text{ends},a}^{\text{eq}} c_d}. \quad \text{[S37d]}$$

Now we insert the relationships above into Eq. (S29a), Eq. (S29c), Eq. (S29e), Eq. (S29g), leading to three kinetic equations for the total mass of monomers  $M_m(t)$ , and the particle concentration of oligomers,  $c_o(t)$ , and the mass and particle concentration of aggregates,  $M_a(t)$  and  $c_a(t)$ , valid in the limit of fast drug binding:

$$-\frac{dM_m(t)}{dt} \simeq \frac{dM_a(t)}{dt} = 2k_+ \left( \frac{M_m(t)}{1 + K_m^{\text{eq}} c_d} \right) \left( \frac{c_a(t)}{1 + K_{\text{ends},a}^{\text{eq}} c_d} \right), \quad \text{[S38a]}$$

$$\begin{aligned} \frac{dc_o(t)}{dt} &= k_1 \left( \frac{M_m(t)}{1 + K_m^{\text{eq}} c_d} \right)^{n_1} + k_2 \left( \frac{M_m(t)}{1 + K_m^{\text{eq}} c_d} \right)^{n_2} \left( \frac{M_a(t)}{1 + K_{\text{surf},a}^{\text{eq}} c_d} \right) \\ &\quad - 2k_{\text{conv}} \left( \frac{M_m(t)}{1 + K_m^{\text{eq}} c_d} \right)^{n_{\text{conv}}} \left( \frac{c_o(t)}{1 + K_o^{\text{eq}} c_d} \right), \end{aligned} \quad \text{[S38b]}$$

$$\frac{dc_a(t)}{dt} = 2k_{\text{conv}} \left( \frac{M_m(t)}{1 + K_m^{\text{eq}} c_d} \right)^{n_{\text{conv}}} \left( \frac{c_o(t)}{1 + K_o^{\text{eq}} c_d} \right). \quad \text{[S38c]}$$

**S2.3.3. Linearized set of equations for fast drug binding and early stage of aggregation with oligomers.** Linearizing Eq. (S38) with the total monomer mass concentration  $M_m(t)$  close to the total protein mass  $M_m^{\text{tot}}$  and considering the initial conditions  $M_a(0) = 0$  and  $c_a(0) = 0$ , we find

$$\frac{dM_a(t)}{dt} \simeq \mu(c_d) c_a(t), \quad \text{[S39a]}$$

$$\frac{dc_o(t)}{dt} \simeq \alpha(c_d) + \beta(c_d) M_a(t) - \gamma(c_d) c_o(t), \quad \text{[S39b]}$$

$$\frac{dc_a(t)}{dt} \simeq \gamma(c_d) c_o(t), \quad \text{[S39c]}$$

where the rates now depend on the drug concentration  $c_d$ :

$$\mu(c_d) = \mu_0 \left( \frac{1}{1 + K_m^{\text{eq}} c_d} \right) \left( \frac{1}{1 + K_{\text{ends},a}^{\text{eq}} c_d} \right), \quad \text{[S40a]}$$

$$\alpha(c_d) = \alpha_0 \left( \frac{1}{1 + K_m^{\text{eq}} c_d} \right)^{n_1}, \quad \text{[S40b]}$$

$$\beta(c_d) = \beta_0 \left( \frac{1}{1 + K_m^{\text{eq}} c_d} \right)^{n_2} \left( \frac{1}{1 + K_{\text{surf},a}^{\text{eq}} c_d} \right), \quad \text{[S40c]}$$

$$\gamma(c_d) = \gamma_0 \left( \frac{1}{1 + K_m^{\text{eq}} c_d} \right)^{n_{\text{conv}}} \left( \frac{1}{1 + K_o^{\text{eq}} c_d} \right). \quad \text{[S40d]}$$

The constant coefficients are defined as  $\mu_0 = 2k_+ M_m^{\text{tot}}$ ,  $\alpha_0 = k_1 (M_m^{\text{tot}})^{n_1}$ ,  $\beta_0 = k_2 (M_m^{\text{tot}})^{n_2}$  and  $\gamma_0 = 2k_{\text{conv}} (M_m^{\text{tot}})^{n_{\text{conv}}}$ .

**S2.3.4. Final kinetic equations with oligomers in the presence of drug and the linear relationship between particle and mass concentration of aggregates.** The linearized equations Eq. (S39) can be written in matrix form

$$\frac{d}{dt} \begin{pmatrix} M_a(t) \\ c_o(t) \\ c_a(t) \end{pmatrix} = \begin{pmatrix} 0 & 0 & \mu \\ \beta & -\gamma & 0 \\ 0 & \gamma & 0 \end{pmatrix} \begin{pmatrix} M_a(t) \\ c_o(t) \\ c_a(t) \end{pmatrix} + \begin{pmatrix} 0 \\ \alpha \\ 0 \end{pmatrix}. \quad [\text{S41}]$$

We are interested in the exponentially growing solutions to Eq. (S41). Thus we search for the largest eigenvalue of the matrix above. The characteristic polynomial for the eigenvalue  $x$  is

$$x^3 + \gamma x^2 - \gamma\beta\mu = 0. \quad [\text{S42}]$$

To find the largest (positive) eigenvalue, we use the method of dominant balance in the limit of small  $\gamma$  (17). The basic idea of this method is to show that two terms of the equation Eq. (S42) balance while the remaining terms vanish as  $\gamma \rightarrow 0$ . The relevant dominant balance for our problem is obtained when

$$x = O(\gamma^{1/3}). \quad [\text{S43}]$$

In fact, writing  $x = \gamma^{1/3}X$  with  $X = O(1)$ , we find

$$X^3 + \gamma^{2/3}X^2 - \beta\mu = 0 \xrightarrow{\gamma \rightarrow 0} X^3 - \beta\mu = 0 \Rightarrow X \simeq (\beta\mu)^{1/3}. \quad [\text{S44}]$$

The largest eigenvalue of interest is therefore approximatively equal to

$$x \simeq (\gamma\beta\mu)^{1/3} \equiv \bar{\kappa}. \quad [\text{S45}]$$

Similar to sections S2.1.1 and S2.2.5 the largest eigenvalue corresponds to the geometrical mean of rates. Due to the exponential growth of all three concentration fields and their circular coupling, the origin of the geometric mean can be illustrated by a so called ‘‘Hinshelwood circle’’ (8). In the case of early stage aggregation with oligomers it is the geometric mean between  $\gamma$ ,  $\beta$  and  $\mu$ , while in the absence of oligomers, the largest eigenvalue is the geometric mean of  $\beta$  and  $\mu$  only.

For  $t \gtrsim \bar{\kappa}$ ,  $M_a(t) \simeq Ae^{\bar{\kappa}t}$ ,  $c_o(t) \simeq Be^{\bar{\kappa}t}$ ,  $c_a(t) \simeq Ce^{\bar{\kappa}t}$ , where  $\bar{\kappa} = (\gamma\beta\mu)^{1/3}$ . Moreover, using Eq. (S39), we find  $A = \mu\gamma/\bar{\kappa}^2$ ,  $C = \gamma/\bar{\kappa}$  and  $B = (\alpha + \gamma\beta\mu/\bar{\kappa}^2)/(\bar{\kappa} + \gamma)$  and

$$M_a(t) \simeq \frac{\mu}{\bar{\kappa}} c_a(t) \simeq \frac{\mu\gamma}{\bar{\kappa}^2} c_o(t). \quad [\text{S46}]$$

Substituting these relationships back into our linearized kinetic equations Eq. (S39), we obtain a single, independent (due to Eq. (S46)) equation describing the aggregation kinetics:

$$\frac{dc_o(t)}{dt} \simeq \alpha + \left( \frac{\gamma\beta\mu}{\bar{\kappa}^2} - \gamma \right) c_o(t) = \alpha(c_d) + \tilde{\kappa}(c_d) c_o(t), \quad [\text{S47}]$$

where  $\tilde{\kappa} = (\gamma\beta\mu/\bar{\kappa}^2) - \gamma = \bar{\kappa} - \gamma$ . The drug dependence of the coefficients are given in Eq. (S40).

Equation Eq. (S47) has the same mathematical form as the kinetic equations for the early stage aggregation in the absence of drug, Eq. (S12), and in the presence of drug solely restricting to large aggregates, Eq. (S28). This mathematical equivalence is only true in the limit of fast drug binding. Of course, the corresponding coefficients are different for each of the mentioned cases. In the next chapter we will use this mathematical similarity and discuss optimal inhibition of irreversible aggregation considering this type of kinetic equation Eq. (S1).

### S3. Optimal inhibition of irreversible aggregation of proteins

We are interested to find the solution to Eq. (S1), which lead to the “optimal” inhibition of aggregates or oligomers, respectively (see Fig. S3(a)). Each solution is characterized by the drug concentration (in general referred to as control). In our case, the drug reduces the amount of aggregates and oligomers. From a naive perspective, the drug level could simply be increased to infinity suppressing all three pathways of aggregation, i.e., primary and secondary nucleation and the growth of the aggregates at their ends (see section S2.2.1). However, the presence of a large amount of drug may be toxic (18). An increase in concentration of a toxic drug competes with an decrease in concentration of aggregates/oligomers that are toxic as well. This competition is mathematically captured by a functional, denoted as “Cost[.]”, which may depend on drug, oligomer and aggregate concentrations. This functional is called “action” (in the context of physics \*) or “cost” (in the context of optimal control theory) and allows to select the “optimal solution”. The optimal solution corresponds to a minimum value of this action/cost functional. It is obtained by minimizing this functional with the constraint that the corresponding controlling drug concentration and aggregate/oligomer concentration are solutions to Eq. (S1). In the next section we will discuss the central equations of this variational problem and apply it to the inhibition of aggregation in the following sections.

**S3.1. Introduction to variational calculus with constraint and optimal control theory .** Let us consider the time dependent control  $c_d(t)$  (e.g. the drug concentration) which controls the solution  $c_a(t)$  to the differential equation

$$\frac{dc_a(t)}{dt} = f(c_d(t), c_a(t)) . \quad [\text{S48}]$$

We aim at the control  $c_d(t)$  that minimizes the “action” or “cost”

$$\text{Cost}[c_d(t), c_a(t)] = \int_0^T dt' \mathcal{L}(c_a(t'), c_d(t')) , \quad [\text{S49}]$$

with the constraint that  $f(c_d(t), c_a(t))$  is a solution to Eq. (S48). Thus we have to minimize the functional

$$\mathcal{F}[c_d(t), c_a(t)] = \text{Cost}[c_d(t), c_a(t)] - \int_0^T dt' \lambda(t') \left( \frac{dc_a(t')}{dt'} - f(c_a(t'), c_d(t')) \right) , \quad [\text{S50}]$$

where  $\lambda(t)$  is a continuous Lagrange multiplier (or co-state variable in the context of optimal control theory) which ensures that the constraint Eq. (S48) is satisfied for all times  $t$ . Minimization yields

$$\delta \mathcal{F}[c_d(t), c_a(t)] = \int_0^T dt' \left( \frac{\delta \mathcal{F}}{\delta c_d} \delta c_d + \frac{\delta \mathcal{F}}{\delta c_a} \delta c_a \right) + \lambda(t) \delta c_a(t) \Big|_0^T . \quad [\text{S51}]$$

The integrated terms on the right hand side vanish for  $\lambda(0) = 0$  and  $\lambda(T) = 0$ , or  $\delta c_a(0) = 0$  and  $\delta c_a(T) = 0$ , or  $\delta c_a(0) = 0$  and  $\lambda(T) = 0$ , or  $\lambda(0) = 0$  and  $\delta c_a(T) = 0$ . With one of these combinations of initial condition at  $t = 0$  and fixed constraint at  $t = T$ , we obtain the following set of equations:

$$0 = \frac{\delta \mathcal{F}}{\delta c_d} = \frac{\partial \mathcal{L}}{\partial c_d} + \lambda(t) \frac{\partial f}{\partial c_d} , \quad [\text{S52a}]$$

$$0 = \frac{\delta \mathcal{F}}{\delta c_a} = \frac{\partial \mathcal{L}}{\partial c_a} + \lambda(t) \frac{\partial f}{\partial c_a} + \frac{d\lambda(t)}{dt} . \quad [\text{S52b}]$$

We have the same number of conditions, Eq. (S52) and Eq. (S48), as unknowns, namely the Lagrange multiplier  $\lambda(t)$ , the solution  $c_a(t)$  and the control  $c_d(t)$ .

The three conditions can be rewritten to establish a “recipe” as commonly presented in textbooks on optimal control theory (19). Defining the “Hamiltonian”

$$\mathcal{H}(c_d(t), c_a(t), \lambda(t)) = \mathcal{L}(c_d(t), c_a(t)) + \lambda(t) f(c_d(t), c_a(t)) , \quad [\text{S53}]$$

Eq. (S52) and Eq. (S48) can be rewritten as

$$\frac{dc_a(t)}{dt} = \frac{\partial \mathcal{H}}{\partial \lambda} , \quad [\text{S54a}]$$

$$\frac{d\lambda(t)}{dt} = - \frac{\partial \mathcal{H}}{\partial c_a} , \quad [\text{S54b}]$$

$$0 = \frac{\partial \mathcal{H}}{\partial c_d} . \quad [\text{S54c}]$$

The defined “Hamiltonian” is conserved along the optimal trajectory, i.e., using Eq. (S54),

$$\frac{d}{dt} \mathcal{H}(c_d(t), c_a(t), \lambda(t)) = \frac{\partial \mathcal{H}}{\partial c_d} \frac{dc_d}{dt} + \frac{\partial \mathcal{H}}{\partial c_a} \frac{dc_a(t)}{dt} + \frac{\partial \mathcal{H}}{\partial \lambda} \frac{d\lambda(t)}{dt} = 0 . \quad [\text{S55}]$$

In the field of optimal control theory, the corresponding mathematical theorem is called Pontryagin minimum principle (PMP) (19). The Pontryagin theorem ensures the existence of a control  $c_d(t)$  characterizing a unique solution  $c_a(t)$  which leads to the smallest value of the Cost[.].

\*Note that we use the term “action” in a broader sense. Here the action not necessarily determines the equation of motions as in the case of Lagrangian mechanics.

**S3.2. Optimal control theory applied to the inhibition of protein aggregation.** To capture the competition between drug-induced inhibition of aggregation,  $c_a(t) \simeq c_o(t)(\gamma/\bar{\kappa})$  (see Eq. (S47)), and the toxic action of the controlling drug concentration,  $c_d(t)$ , we introduce the following functional called “cost” or “action”,

$$\text{Cost}[c_d, c_a] = \int_0^T dt \left( c_a(t) + \zeta c_d(t) \right), \quad [\text{S56}]$$

where we consider a linear dependence on the concentrations for simplicity. We introduce a toxicity  $\zeta$  for the drug measured relative to the toxicity to the large aggregates (a) or oligomers (o), respectively. Note that the amplitude of the cost functional,  $\text{Cost}[\cdot]$ , does not matter for results obtained by variational calculus. The cost above increases for larger time periods  $T$  and for higher concentrations of drug and aggregates and oligomers. Increasing the drug concentration creates extra “costs” for the cell, to degrade the drug and/or maintain the biological function the cellular machinery in the presence of the drug for example. Similarly, too many aggregates/oligomers also increase these cellular costs.

Alternatively, the presence of aggregates/oligomers for  $t < T$  may not create any costs for the cell, while there is a “terminal cost” at  $t = T$ ,

$$\text{Cost}[c_d, c_a(T)] = T c_a(T) + \int_0^T dt \zeta c_{d,i}(t). \quad [\text{S57}]$$

In the following we will study both cases of integrated cost (Eq. (S56)) and terminal cost (Eq. (S57)) as they may represent limiting cases for a living system in which aggregates may cause both type of costs. For the considered equation Eq. (S1), however, we will see that there is no qualitative difference in the results between integrated and terminal costs.

By means of the cost function we can select the optimal solution set by the drug concentration  $c_d(t)$ . This drug inhibits protein aggregation by at least one of the mechanisms discussed in section S2.2.1, by some combination of them or via all three mechanisms. To solve the optimal control problem described in the last section, we apply the variational recipe as introduced in section S3.1. To this end, we introduce the Lagrange multiplier or co-state variable  $\lambda(t)$  and define the following Hamiltonian in the case of integrated costs (Eq. (S56)),

$$\mathcal{H}[c_d(t), c_a(t), \lambda(t)] = c_a(t) + \zeta c_d(t) + \lambda(t) \left[ \alpha(c_d(t)) + \kappa(c_d(t)) c_a(t) \right], \quad [\text{S58}]$$

while for terminal costs (Eq. (S57)), the Hamiltonian reads

$$\mathcal{H}[c_d(t), c_a(t), \lambda(t)] = \zeta c_d(t) + \lambda(t) \left[ \alpha(c_d(t)) + \kappa(c_d(t)) c_a(t) \right]. \quad [\text{S59}]$$

The evolution equation for the Lagrange multiplier or co-state variable  $\lambda(t)$  is

$$\frac{d\lambda(t)}{dt} = -\frac{\partial \mathcal{H}}{\partial c_a} = -1 - \kappa(c_d) \lambda(t). \quad [\text{S60}]$$

Since the concentration of aggregates at  $t = T$  is free, we solve Eq. (S60) subject to the condition

$$\lambda(T) = A, \quad [\text{S61}]$$

which is referred to as transversality condition in the context of optimal control theory (19). Here,  $A$  is a constant. In particular,  $A = 0$  for integrated costs (Eq. (S56)) and  $A = T$  for terminal costs (Eq. (S57)). By construction, the kinetic equation for the drug concentration reads

$$\frac{dc_a(t)}{dt} = \frac{\partial \mathcal{H}}{\partial \lambda} = \alpha(c_d(t)) + \kappa(c_d(t)) c_a(t). \quad [\text{S62}]$$

The optimal control can be calculated by the condition

$$\frac{\partial \mathcal{H}}{\partial c_d} = 0, \quad [\text{S63}]$$

i.e., the optimal drug concentration  $c_d(t)$  corresponds to a minimum of the Hamiltonian with respect to the drug concentration. If the drug concentration were a continuous concentration profile, the condition for the minimum is given in equation Eq. (S63). However, the drug concentration may jump at the times  $T_1$  and  $T_2$  (see Eq. (S67) in the next section). Therefore, the derivatives of the rates  $\kappa(c_d)$  and  $\alpha(c_d)$  with respect to  $c_d$  jump as well, i.e.,  $\kappa' = (\kappa(c_d) - \kappa_0)/c_d$  and  $\alpha' = (\alpha(c_d) - \alpha_0)/c_d$ . The minimum condition gives different conditions at  $t = T_i$ ,

$$\frac{\partial \mathcal{H}}{\partial c_d} = \zeta + \lambda(T_i) \left[ \alpha' + \kappa' c_a(T_i) \right] = 0, \quad [\text{S64}]$$

where the times  $T_i$  are determined by the actual drug protocol which we discuss in the following section.

**S3.3. Drug protocols for optimal inhibition.** To discuss the drug protocol we consider the case of zero aggregates at time  $t = 0$ ,

$$c_a(0) = 0, \quad [\text{S65}]$$

i.e., the patient is initially healthy.

The drug concentration in Eq. (S1) is constant in the limit of fast binding of the drug to the aggregates and the monomers (see sections S2.2.3 and S2.3.2). Consistently, we can only use a constant concentration for the drug. However, concentration levels may be different in different time spans of the treatment. Depending on the value of the toxicity  $\zeta$  and the kinetic parameters,  $\alpha$  and  $\kappa$ , there are two different type of drug protocols (see Fig. S3(d,e) on the right hand side). Each drug protocol can be derived from the minimization of the Hamiltonian, Eq. (S64), which can be written as

$$\zeta = \lambda(T_i) (|\alpha'| + |\kappa'| c_a(T_i)), \quad [\text{S66}]$$

noting that  $\alpha'(c_d) < 0$  and  $\kappa'(c_d) < 0$  (see e.g. Eq. (S27b) and Eq. (S27d)). This condition either yields two solutions,  $T_1$  and  $T_2$ , or just one,  $T_2$  (see Fig. S3(b,c,d,e)). The corresponding protocols either read

$$c_d(t) = \begin{cases} 0 & \text{for } 0 \leq t < T_1, \\ c_d & \text{for } T_1 \leq t < T_2, \\ 0 & \text{for } T_2 \leq t \leq T, \end{cases} \quad [\text{S67}]$$

or

$$c_d(t) = \begin{cases} c_d & \text{for } 0 \leq t < T_2, \\ 0 & \text{for } T_2 \leq t \leq T, \end{cases} \quad [\text{S68}]$$

where  $T_1$  or  $t = 0$ , respectively, is the time of drug administration,  $T_2 - T_1$  or just  $T_2$  denotes the time period the drug is applied, and  $T - T_2$  is a drug-free period after medication.

In the following we compare two different physical scenarios, where each corresponds to the drug protocol Eq. (S67) or Eq. (S68), respectively:

- 1) The first scenario is the case where primary nucleation is not affected by the drug, i.e.,  $\alpha(c_d) = \alpha_0$ ; the drug only decreases secondary nucleation and growth at the ends of the aggregates. This case leads to the drug protocol Eq. (S67) illustrated in Fig. S3(d).
- 2) The second scenario corresponds to  $\kappa(c_d) = \kappa_0$ , i.e., secondary nucleation and growth at the ends are not affected by the drug. Instead the drug only inhibits primary nucleation. This case leads to the drug protocol Eq. (S68) illustrated in Fig. S3(e).

Later we will determine the parameter regimes where one of these strategies is more efficient to inhibit protein aggregation than the other. The optimal protocol for a drug inhibiting multiple aggregation steps can be obtained explicitly by solving Eq. (S66) and is a combination of the scenarios (1) and (2) discussed here below.

**S3.4. Optimal inhibition.** We seek for the optimal treatment leading to the most effective inhibition of aggregate growth. We would like optimize the treatment, characterized by the times  $T_1$  and  $T_2$  and the drug concentration  $c_d$ , such that the aggregate concentration  $c_a(t = T)$  at the final time  $t = T$  is an output of the optimization procedure. Thus we let the final aggregate concentration  $c_a(t = T)$  “free” and fix the final time  $T$ , which corresponds to the condition Eq. (S61).

The optimal drug treatment can be found by calculating the optimal times to begin,  $T_1$ , and to end the drug treatment,  $T_2$ , which minimize the cost functional Eq. (S56) given the aggregation kinetics governed by Eq. (S28).

By means of the optimization we will determine the weakest and optimal growth of the concentration of aggregates,  $c_a(t)$ , and oligomers,  $c_o(t)$ ; see section S3.4.1. We calculate the dependencies of the times to begin,  $T_1$ , and end,  $T_2$ , the drug treatment as a function of the aggregation parameters and the relative toxicities  $\zeta$  (section Eq. (S3.4.2)). These results will allow us to discuss how the life time expectance of patients is decreased if the treatment deviates from the optimum or if there is no drug treatment (section S3.4.5).

**S3.4.1. Solutions for Lagrange multiplier (co-state variable) and solution to aggregation kinetics.** For  $T_2 \leq t \leq T$ , we solve Eq. (S60) considering that  $c_d(t = T) = 0$  and thus  $\kappa(c_d = 0) = \kappa_0$  (see Eq. (S67)):

$$\lambda(t) = \frac{e^{\kappa_0(T-t)} - 1}{\kappa_0} + A e^{\kappa_0(T-t)}, \quad T_2 \leq t \leq T. \quad [\text{S69a}]$$

To obtain the solution in the time period  $T_1 \leq t < T_2$ , we solve Eq. (S60) with  $c_d = c_d$ , and match with the solution above at  $t = T_2$ :

$$\lambda(t) = \frac{e^{\kappa(c_d)[T_2-t]} - 1}{\kappa(c_d)} + \lambda(T_2) e^{\kappa(c_d)[T_2-t]}, \quad T_1 \leq t < T_2. \quad [\text{S69b}]$$

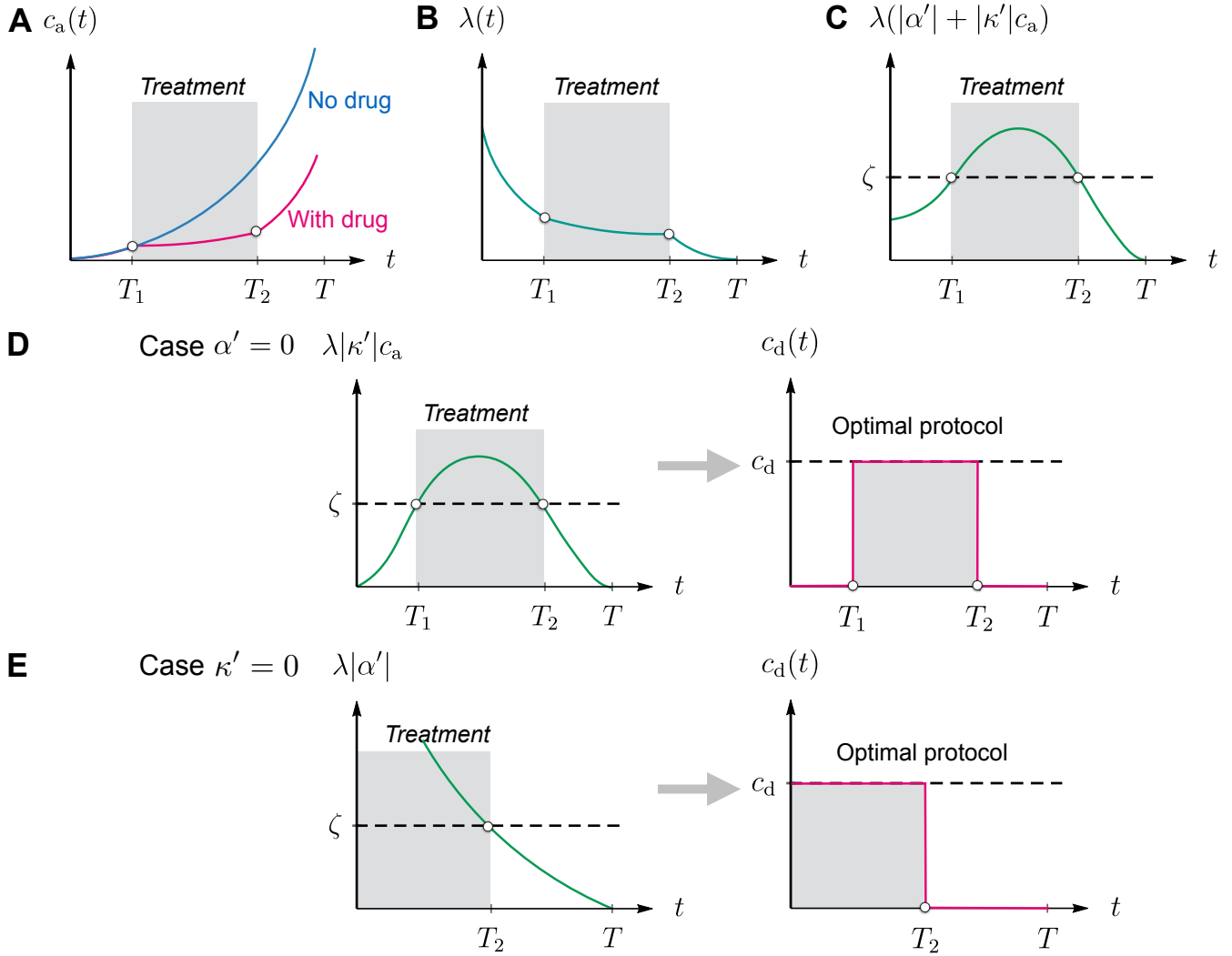


**Fig. S3.** (a) Effect of optimal control on aggregate concentration. While the aggregate concentration  $c_a(t)$  grows exponentially in time in the absence of drug, a drug treatment within the time interval  $[T_1, T_2]$  can significantly inhibit the aggregate growth. (b) Sketch of time evolution of co-state variable  $\lambda(t)$  with the transversality condition  $\lambda(T) = 0$  (in the case of integrated costs). Please refer to section S3.4.1 for the solutions of co-state variable  $\lambda(t)$  as a function of time. (c) Illustration of the time evolution of the quantity  $\lambda(t)[|\alpha'| + |\kappa'|c_a(t)]$  which essentially determines the drug protocol. Note that  $\lambda(t)[|\alpha'| + |\kappa'|c_a(t)]$  is the product of  $\lambda(t)$  (monotonically decreasing; see section S3.4.1) and  $|\alpha'| + |\kappa'|c_a(t)$  (monotonically increasing or constant; see section S3.4.1), hence it can have a non-monotonic behavior. The switching times  $T_1$  and  $T_2$  are set by the condition Eq. (S66). (d) Optimal protocol for the case  $\alpha' = 0$ . Drug is administered at  $t = T_1 > 0$  with the drug protocol Eq. (S67) illustrated on the right hand side. (e) Optimal protocol for the case  $\kappa' = 0$ . Drug is administered already at  $t = 0$  with the drug protocol Eq. (S68) illustrated to the right.

For  $0 \leq t < T_1$ , we find:

$$\lambda(t) = \frac{e^{\kappa_0(T_1-t)} - 1}{\kappa_0} + \lambda(T_1) e^{\kappa_0(T_1-t)}, \quad 0 \leq t < T_1. \quad [\text{S69c}]$$

Please refer to Fig. S3(b) for an illustration of  $\lambda(t)$ . Since we have fixed the form of the drug as a function of time  $c_a(t)$  (Eq. (S67)), we can already calculate of the optimal concentration of aggregates as a function of time,  $c_a(t)$ , governed by

$$\frac{dc_a(t)}{dt} = \frac{\partial \mathcal{H}}{\partial \lambda} = \alpha(c_d) + \kappa(c_d) c_a(t). \quad [\text{S70}]$$

Using the initial condition  $c_a(0) = 0$ , we find:

$$c_a(t) = \frac{\alpha_0}{\kappa_0} [e^{\kappa_0 t} - 1], \quad 0 \leq t \leq T_1, \quad [\text{S71a}]$$

$$c_a(t) = \frac{\alpha(c_d)}{\kappa(c_d)} \left[ e^{\kappa(c_d)[t-T_1]} - 1 \right] + c_a(T_1) e^{\kappa(c_d)[t-T_1]}, \quad T_1 < t \leq T_2, \quad [\text{S71b}]$$

$$c_a(t) = \frac{\alpha_0}{\kappa_0} \left[ e^{\kappa_0[t-T_2]} - 1 \right] + c_a(T_2) e^{\kappa_0[t-T_2]}, \quad T_2 < t \leq T. \quad [\text{S71c}]$$

Note that in the absence of any drug treatment,

$$c_a(t) = \frac{\alpha_0}{\kappa_0} [e^{\kappa_0 t} - 1], \quad 0 \leq t \leq T. \quad [\text{S72}]$$

Please refer to Fig. S3(a) for an illustration of how the concentration of aggregates changes with time, in the presence and absence of drug.

**S3.4.2. Optimal start and end of drug treatment.** So far we have not yet determined the optimal values for the times to begin,  $T_1$ , and to end the drug treatment,  $T_2$ . To this end, we consider the two cases outlined in section S3.3.

- *Case  $\alpha(c_d) = \alpha_0$  and  $\alpha' = 0$  corresponding to the drug protocol Eq. (S67):*

Using Eq. (S69) and Eq. (S71), we find

$$-\zeta = \left[ \frac{e^{\kappa[T_2-T_1]} - 1}{\kappa} + \frac{\Gamma e^{\kappa_0(T-T_2)} - 1}{\kappa_0} e^{\kappa[T_2-T_1]} \right] \kappa' \frac{\alpha_0}{\kappa_0} (e^{\kappa_0 T_1} - 1), \quad [\text{S73a}]$$

$$-\zeta = \left[ \frac{\Gamma e^{\kappa_0(T-T_2)} - 1}{\kappa_0} \right] \left[ \kappa' \frac{\alpha_0}{\kappa} (e^{\kappa[T_2-T_1]} - 1) + \kappa' \frac{\alpha_0}{\kappa_0} (e^{\kappa_0 T_1} - 1) e^{\kappa[T_2-T_1]} \right], \quad [\text{S73b}]$$

where we have suppressed the dependence on  $c_d$  of  $\kappa$  for the ease of notation, i.e.,  $\kappa = \kappa(c_d)$ . Moreover, we have introduced the following abbreviation

$$\Gamma(A) = 1 + \kappa_0 A, \quad [\text{S74}]$$

where  $A = 0$ , i.e.,  $\Gamma = 1$  for integrated cost (Eq. (S56)) and  $A = T$  for terminal cost (Eq. (S57)).

The equations above determine the optimal values for  $T_1$  and  $T_2$ . To obtain an analytic result, we consider the case where  $T_i \ll \kappa^{-1}$ . This condition has already been used to derive the underlying kinetic equation for aggregation (see section S2.2.5). In particular, this implies that  $e^{\kappa T_i} \gg 1$ . The resulting two equations can be subtracted or added, respectively, leading to

$$T - T_2 \simeq T_1 - \frac{1}{\kappa_0} \ln(\Gamma), \quad [\text{S75a}]$$

$$T_2 - T_1 \simeq \frac{1}{\kappa_0 - \kappa} \left[ T \kappa_0 - \ln \left( \frac{\zeta \kappa_0^2 c_d}{\alpha_0 (\kappa_0 - \kappa) \Gamma} \right) \right]. \quad [\text{S75b}]$$

Eq. (S75b) describes the optimal treatment period ( $T_2 - T_1$ ). The expression for the treatment period  $T_2 - T_1$  (Eq. (S75b)) indeed minimizes the cost (see next section). Depending on the parameters such as relative toxicity  $\zeta$  or aggregation rates, there is a regime at large toxicity where a drug treatment makes no sense since the drug is too toxic. In the case of a drug of low toxicity, the optimal treatment duration approaches  $T$ . For integrated cost, the drug administration protocol is symmetric, i.e.  $T - T_2 = T_1$ . The start and end times are then explicitly given by:

$$T_1 \simeq \frac{T}{2} - \frac{1}{2(\kappa_0 - \kappa)} \left[ T \kappa_0 - \ln \left( \frac{\zeta \kappa_0^2 c_d}{\alpha_0 (\kappa_0 - \kappa) \Gamma} \right) \right], \quad [\text{S76a}]$$

$$T_2 \simeq \frac{T}{2} + \frac{1}{2(\kappa_0 - \kappa)} \left[ T \kappa_0 - \ln \left( \frac{\zeta \kappa_0^2 c_d}{\alpha_0 (\kappa_0 - \kappa) \Gamma} \right) \right]. \quad [\text{S76b}]$$

No treatment is preferable when  $T_2 < T_1$ , i.e. when

$$T \kappa_0 - \ln \left( \frac{\zeta \kappa_0^2 c_d}{\alpha_0 (\kappa_0 - \kappa) \Gamma} \right) < 0 \quad \Rightarrow \quad c_d > \frac{\alpha_0 (\kappa_0 - \kappa) \Gamma}{\zeta \kappa_0^2} e^{\kappa_0 T} \simeq \frac{\alpha_0 \Gamma}{\zeta \kappa_0} e^{\kappa_0 T}. \quad [\text{S77}]$$



- *Case  $\kappa(c_d) = \kappa_0$  and  $\kappa' = 0$  corresponding to the drug protocol Eq. (S68):*

Following the analog steps as sketched in the previous paragraph, we find for the switching time  $T_2$  for the optimal inhibition of primary nucleation.  $T_2$  is obtained as solution to (Fig. S3(e)):

$$\zeta = \lambda(T_2) |\alpha'|, \quad [\text{S78}]$$

where  $\lambda(t)$  is given by

$$\lambda(t) = \frac{e^{\kappa_0(T-t)} - 1}{\kappa_0} + A e^{\kappa_0(T-t)}. \quad [\text{S79}]$$

Hence,

$$T_2 = T - \frac{1}{\kappa_0} \ln \left[ \Gamma^{-1} \left( \frac{\zeta \kappa_0 c_d}{\alpha_0 - \alpha(c_d)} + 1 \right) \right] \simeq T - \frac{1}{\kappa_0} \ln \left( \frac{\zeta \kappa_0 c_d}{(\alpha_0 - \alpha(c_d)) \Gamma} \right). \quad [\text{S80}]$$

In this case, no treatment is preferable when  $T_2 < 0$ , i.e. when

$$c_d > \frac{(\alpha_0 - \alpha) \Gamma}{\zeta \kappa_0} e^{\kappa_0 T} \simeq \frac{\alpha_0 \Gamma}{\zeta \kappa_0} e^{\kappa_0 T}. \quad [\text{S81}]$$

**S3.4.3. Optimal costs and treatments deviating from the optimum.** Here we compute the cost as the treatment deviates from the optimum to estimate the additional “life time” gained by the optimization. One limiting case is no drug treatment. Using Eq. (S72) and the definition of the cost Eq. (S56) for a single drug, we find the cost in the absence of drug treatment

$$\text{Cost}_\times \simeq \frac{\alpha_0}{\kappa_0^2} e^{\kappa_0 T}. \quad [\text{S82}]$$

To calculate the cost with treatment, we consider the contributions from the drug and from the aggregates separately. For the drug, the cost is given as:

$$\text{Cost}[0, c_d] = \int_0^T dt \zeta c_d(t) = \zeta c_d(T_2 - T_1). \quad [\text{S83}]$$

The optimized contribution from the drug is obtained by using Eq. (S75b):

$$\begin{aligned} \text{Cost}_{\text{opt}}[0, c_d] &= \frac{\zeta c_d}{\kappa_0 - \kappa} \left[ T \kappa_0 - \ln \left( \frac{\zeta \kappa_0^2 c_d}{\alpha_0 (\kappa_0 - \kappa) \Gamma} \right) \right] \\ &= \zeta \phi(c_d) \left[ T - \frac{1}{\kappa_0} \ln \left( \frac{\zeta \kappa_0 \phi(c_d)}{\alpha_0 \Gamma} \right) \right], \end{aligned} \quad [\text{S84}]$$

where

$$\phi(c_d) = \frac{c_d \kappa_0}{\kappa_0 - \kappa} = \frac{c_d}{1 - 1/(1 + c_d K)^n} = \begin{cases} c_d & c_d \gg K^{-1} \\ \frac{1}{nK} + \frac{n+1}{2n} c_d & c_d \ll K^{-1} \end{cases}, \quad [\text{S85}]$$

where  $K$  is the equilibrium binding constant of the drug via some of the discussed mechanisms and  $n$  is some exponent (which depends on the reaction orders for nucleation and the mechanism of inhibition etc.). For the cost from the aggregates, we consider the two cases outlined in section S3.3 separately.

*Case  $\alpha(c_d) = \alpha_0$  and  $\alpha' = 0$  corresponding to the drug protocol Eq. (S67):*

The cost of the aggregates will slightly differ between of integrated and terminal costs. In the case of integrated cost

$$\begin{aligned} \text{Cost}[c_a, 0] &= \int_0^T dt c_a(t) = \int_0^{T_1} dt c_a(t) + \int_{T_1}^{T_2} dt c_a(t) + \int_{T_2}^T dt c_a(t) \\ &\simeq \frac{\alpha_0}{\kappa_0^2} e^{\kappa_0 T_1} e^{\kappa(T_2 - T_1)} e^{\kappa_0(T - T_2)} = \frac{\alpha_0}{\kappa_0^2} e^{\kappa_0 T} \cdot e^{-(\kappa_0 - \kappa)(T_2 - T_1)}, \end{aligned} \quad [\text{S86}]$$

where we extracted the dominant exponential terms in  $c_a(t)$ . The optimized contribution from the aggregates is found by using Eq. (S75a) and Eq. (S75b):

$$\text{Cost}_{\text{opt}}[c_a, 0] \simeq \frac{\zeta}{|\kappa'|} = \frac{\zeta}{\kappa_0} \phi(c_d). \quad [\text{S87}]$$

In the case of terminal costs (see Eq. (S57)), the costs from the aggregates reads  $\text{Cost}[c_a, 0] = T c_a(T)$  and the optimized contribution using Eq. (S74) is

$$\text{Cost}_{\text{opt}}[c_a, 0] = \frac{\kappa_0 T \zeta}{|\kappa'| \Gamma(A = T)} = \frac{T \zeta}{1 + \kappa_0 T} \phi(c_d). \quad [\text{S88}]$$

Due to the exponential growth, integrated and terminal costs only differ by a multiplicative factor. So we focus on integrated cost with  $\Gamma = 1$  (Eq. (S74)) for the remaining discussions without the loss of generality.

In the case of integrated the total cost is is approximately given as

$$\begin{aligned} \text{Cost}[c_a, c_d] &= \text{Cost}[0, c_d] + \text{Cost}[c_a, 0] \\ &\simeq \zeta c_d (T_2 - T_1) + \frac{\alpha_0}{\kappa_0^2} e^{\kappa_0 T} \cdot e^{-(\kappa_0 - \kappa)(T_2 - T_1)}, \end{aligned} \quad [\text{S89}]$$

and the corresponding optimized cost is

$$\begin{aligned} \text{Cost}_{\text{opt}}[c_a, c_d] &= \text{Cost}_{\text{opt}}[0, c_d] + \text{Cost}_{\text{opt}}[c_a, 0] \\ &\simeq \zeta \phi(c_d) \left[ T + \frac{1}{\kappa_0} - \frac{1}{\kappa_0} \ln \left( \frac{\zeta \kappa_0 \phi(c_d)}{\alpha_0 \Gamma} \right) \right]. \end{aligned} \quad [\text{S90}]$$

Case  $\kappa(c_d) = \kappa_0$  and  $\kappa' = 0$  corresponding to the drug protocol Eq. (S68):

Following similar steps as outlined above we find for the total cost

$$\text{Cost}[c_a, c_d] \simeq \frac{\alpha_0 - \alpha}{\kappa_0^2} e^{\kappa_0(T - T_2)} + \frac{\alpha}{\kappa_0^2} e^{\kappa_0 T} + \zeta c_d T_2. \quad [\text{S91}]$$

The optimal cost is then

$$\text{Cost}_{\text{opt}} \simeq \frac{\alpha}{\kappa_0^2} e^{\kappa_0 T} + \zeta c_d \left[ T + \frac{1}{\kappa_0} - \frac{1}{\kappa_0} \ln \left( \frac{\zeta \kappa_0 c_d}{\alpha_0 - \alpha} \right) \right] + \frac{\alpha_0 - \alpha}{\kappa_0^2}. \quad [\text{S92}]$$

**S3.4.4. Sensitivity of optimal control.** Here we discuss the sensitivity to find the optimal treatment. As an example we restrict ourselves to the case  $\alpha(c_d) = \alpha_0$  and  $\alpha' = 0$  corresponding to the drug protocol Eq. (S67) and integrated costs.

The cost function is given by Eq. (S89):

$$\text{Cost}[c_a, c_d] = \zeta c_d (T_2 - T_1) + \frac{\alpha_0}{\kappa_0^2} e^{\kappa_0 T} \cdot e^{-(\kappa_0 - \kappa)(T_2 - T_1)}. \quad [\text{S93}]$$

Minimization of this cost function with respect to treatment duration,  $T_2 - T_1$ , i.e.,

$$\frac{\partial \text{Cost}[c_a, c_d]}{\partial (T_2 - T_1)} = \zeta c_d - \frac{\alpha_0 (\kappa_0 - \kappa)}{\kappa_0^2} e^{\kappa_0 T} \cdot e^{-(\kappa_0 - \kappa)(T_2 - T_1)} = 0, \quad [\text{S94}]$$

yields the optimal treatment duration

$$T_2 - T_1 = \frac{1}{\kappa_0 - \kappa} \left[ \kappa_0 T - \ln \left( \frac{\zeta \kappa_0^2 c_d}{\alpha_0 (\kappa_0 - \kappa)} \right) \right], \quad [\text{S95}]$$

which, consistently, is equivalent to Eq. (S75b) obtained by the optimal control recipe. In addition, we can determine the curvature of the cost function,

$$\frac{\partial^2 \text{Cost}[c_a, c_d]}{\partial (T_2 - T_1)^2} = \frac{\alpha_0 (\kappa_0 - \kappa)^2}{\kappa_0^2} e^{\kappa_0 T} \cdot e^{-(\kappa_0 - \kappa)(T_2 - T_1)},$$

which reads at the optimal treatment duration (Eq. (S75b)):

$$\left. \frac{\partial^2 \text{Cost}[c_a, c_d]}{\partial (T_2 - T_1)^2} \right|_{\text{opt}} = (\kappa_0 - \kappa(c_d)) \zeta c_d.$$

Hence, at low drug concentration  $c_d$  or low drug toxicity  $\zeta$ , the curvature of the cost function at the optimal treatment is smaller. A low curvature around the optimal treatment implies that the optimal treatment is easier to find. In other words, at low toxicity or drug concentration, the optimal treatment is less sensitive to deviations from the optimal value.

**S3.4.5. Life-time expectancy.** By means of the cost function we can discuss how the life time expectancy, denoted as  $T^{\text{life}}$ , changes as the treatment is not optimal or in the case without drug treatment. To define the life expectancy, we introduce a critical value of the cost,  $\text{Cost}_c$ . If the the cost is above this critical value, the cell (for example) dies. Without drug treatment (use Eq. (S82)), we find that the life expectancy is

$$T_{\times}^{\text{life}} = \frac{1}{\kappa_0} \ln \left( \frac{\text{Cost}_c \kappa_0^2}{\alpha_0} \right). \quad [\text{S96}]$$

Similarly, the life expectancies  $T^{\text{life}}$  with drug treatment of optimized duration and fixed drug concentration is determined by:

$$\text{Cost}_c \simeq \zeta \phi(c_d) \left[ T^{\text{life}} + \frac{1}{\kappa_0} - \frac{1}{\kappa_0} \ln \left( \frac{\zeta \kappa_0 \phi(c_d)}{\alpha_0 \Gamma} \right) \right], \quad [\text{S97}]$$

where we used Eq. (S90) thus considered the case  $\alpha(c_d) = \alpha_0$  and  $\alpha' = 0$  corresponding to the drug protocol Eq. (S67)). The life time gain by an optimized drug treatment relative to no treatment is then given as

$$T^{\text{life}} - T_{\times}^{\text{life}} \simeq \frac{\text{Cost}_c}{\zeta \phi(c_d)} - \frac{1}{\kappa_0} + \frac{1}{\kappa_0} \ln \left( \frac{\zeta \phi(c_d)}{\kappa_0 \Gamma \text{Cost}_c} \right). \quad [\text{S98}]$$

**S3.4.6. Comparing strategies: Inhibition of primary nucleation against inhibition of secondary nucleation and growth at ends.** Interestingly, Eq. (S92) shows that targeting the primary nucleation pathway only does not get rid of the exponential term  $e^{\kappa_0 T}$  in the total cost. This is in contrast to the situation when  $\kappa$  is targeted (see Eq. (S90)). Thus, we expect that for large  $\kappa_0 T$  targeting primary nucleation only is more costly than targeting  $\kappa$ . This observation can be formalised by comparing Eq. (S92) with Eq. (S90) finding that affecting primary nucleation only is more favourable than targeting  $\kappa$  when the cost associated with the inhibition of primary nucleation is lower than that associated with the inhibition of secondary nucleation:

$$\begin{aligned} & \frac{\alpha}{\kappa_0^2} e^{\kappa_0 T} + \zeta c_d \left[ T + \frac{1}{\kappa_0} - \frac{1}{\kappa_0} \ln \frac{\zeta \kappa_0 c_d}{(\alpha_0 - \alpha)} \right] + \frac{\alpha_0 - \alpha}{\kappa_0^2} \\ & < \zeta c_d \frac{\kappa_0}{\kappa_0 - \kappa} \left[ T + \frac{1}{\kappa_0} - \frac{1}{\kappa_0} \ln \left( \frac{\zeta \kappa_0^2 c_d}{\alpha_0 (\kappa_0 - \kappa)} \right) \right]. \end{aligned} \quad [\text{S99}]$$

We can simplify the above expression for  $\frac{\alpha_0 - \alpha}{\kappa_0^2} \ll e^{\kappa_0 T}$ ,  $\ln(\dots) \ll \kappa_0 T \ll 1$ , leading to:

$$\frac{\alpha}{\kappa_0^2} e^{\kappa_0 T} + \zeta c_d T < \frac{\zeta c_d \kappa_0 T}{\kappa_0 - \kappa}. \quad [\text{S100}]$$

Hence, inhibiting primary nucleation is to be preferred over the inhibition of secondary nucleation when:

$$\frac{e^{\kappa_0 T}}{\kappa_0 T} < \frac{\zeta c_d \kappa}{\kappa_0 - \kappa} \frac{\kappa_0}{\alpha} \simeq \frac{\zeta c_d \kappa}{\alpha}. \quad [\text{S101}]$$

**S3.5. Optimal drug concentration.** For a fixed treatment duration, the cost function exhibits a minimum as a function of drug concentration. For the inhibition of primary nucleation, the optimal drug concentration is obtained by minimizing

$$\text{Cost}[c_a, c_d] \simeq \frac{\alpha_0 - \alpha}{\kappa_0^2} e^{\kappa_0(T-T_2)} + \frac{\alpha}{\kappa_0^2} e^{\kappa_0 T} + \zeta c_d T_2. \quad [\text{S102}]$$

with respect to  $c_d$ , while for the inhibition of secondary nucleation or fibril elongation, it emerges from the minimization of

$$\text{Cost}[c_a, c_d] = \zeta c_d (T_2 - T_1) + \frac{\alpha_0}{\kappa_0^2} e^{\kappa_0 T - (\kappa_0 - \kappa)(T_2 - T_1)}. \quad [\text{S103}]$$

**S3.6. Optimal controls for pre-aged systems: role of initial concentration.** So far, we have focussed on the situation when the initial aggregate concentration is zero, i.e. the patient is initially healthy (see Eq. (S65)). We now relax this assumption and compute the optimal drug administration protocol when

$$c_a(0) = c_a^0 \quad [\text{S104}]$$

This situation corresponds to patients that are pre-aged in terms of progression of aggregation. Our goal is to understand how an initial concentration of aggregates impacts the optimal drug administration protocol. With this understanding we can decide which inhibition strategy (inhibition of primary respectively secondary nucleation) is preferred depending on the initial concentration of aggregates, i.e. the level of pre-ageing in the patient. We follow the same conceptual steps as in Secs. S3.2-S3.4. For simplicity, we focus on the situation when  $\Gamma = 1$  (integrated cost).

**S3.6.1. Optimal control.** In the presence of an initial concentration of aggregates, the solution for the aggregate concentration is (see Eq. (S71) for comparison):

$$c_a(t) = \frac{\alpha_0}{\kappa_0} [e^{\kappa_0 t} - 1] + c_a^0 e^{\kappa_0 t}, \quad 0 \leq t \leq T_1, \quad [\text{S105a}]$$

$$c_a(t) = \frac{\alpha(c_d)}{\kappa(c_d)} \left[ e^{\kappa(c_d)[t-T_1]} - 1 \right] + c_a(T_1) e^{\kappa(c_d)[t-T_1]}, \quad T_1 < t \leq T_2, \quad [\text{S105b}]$$

$$c_a(t) = \frac{\alpha_0}{\kappa_0} \left[ e^{\kappa_0[t-T_2]} - 1 \right] + c_a(T_2) e^{\kappa_0[t-T_2]}, \quad T_2 < t \leq T. \quad [\text{S105c}]$$

Using Eq. (S69) and Eq. (S105), we find the condition for the optimal switching times as (see Eq. (S106) for comparison):

$$-\zeta = \left[ \frac{e^{\kappa[T_2-T_1]} - 1}{\kappa} + \frac{\Gamma e^{\kappa_0(T-T_2)} - 1}{\kappa_0} e^{\kappa[T_2-T_1]} \right] \kappa' \left[ \frac{\alpha_0}{\kappa_0} (e^{\kappa_0 T_1} - 1) + c_a^0 e^{\kappa_0 T_1} \right], \quad [\text{S106a}]$$

$$-\zeta = \left[ \frac{\Gamma e^{\kappa_0(T-T_2)} - 1}{\kappa_0} \right] \left[ \kappa' \frac{\alpha_0}{\kappa} (e^{\kappa[T_2-T_1]} - 1) + \kappa' \left( \frac{\alpha_0}{\kappa_0} (e^{\kappa_0 T_1} - 1) + c_a^0 e^{\kappa_0 T_1} \right) e^{\kappa[T_2-T_1]} \right], \quad [\text{S106b}]$$

The resulting two equations in Eq. (S106) can be subtracted, leading to

$$T_1 = T - T_2 - \frac{1}{\kappa_0} \ln \left( 1 + \frac{\kappa_0 c_a^0}{\alpha_0} \right). \quad [\text{S107}]$$

Adding the two equations in Eq. (S106) leads to the condition (see Eq. (S75a)):

$$\kappa_0 T_1 + \kappa(T_2 - T_1) + \kappa_0(T - T_2) = \ln\left(\frac{\zeta \kappa_0^2 c_d}{\alpha_0(\kappa_0 - \kappa)}\right) - \ln\left(1 + \frac{\kappa_0 c_a^0}{\alpha_0}\right) \quad [\text{S108}]$$

such that, using Eq. (S107), the optimal switching times can be calculated to be

$$T_1 \simeq \frac{T}{2} - \frac{1}{2(\kappa_0 - \kappa)} \left[ T\kappa_0 - \ln\left(\frac{\zeta \kappa_0^2 c_d}{\alpha_0(\kappa_0 - \kappa)\Gamma}\right) \right] - \frac{1}{\kappa_0} \left(1 + \frac{\kappa}{2(\kappa_0 - \kappa)}\right) \ln\left(1 + \frac{\kappa_0 c_a^0}{\alpha_0}\right), \quad [\text{S109a}]$$

$$T_2 \simeq \frac{T}{2} + \frac{1}{2(\kappa_0 - \kappa)} \left[ T\kappa_0 - \ln\left(\frac{\zeta \kappa_0^2 c_d}{\alpha_0(\kappa_0 - \kappa)\Gamma}\right) \right] + \frac{\kappa}{2\kappa_0(\kappa_0 - \kappa)} \ln\left(1 + \frac{\kappa_0 c_a^0}{\alpha_0}\right). \quad [\text{S109b}]$$

Hence, in the presence of an initial concentration of aggregates,  $T_1$  is decreased and  $T_2$  is increased (Fig. S4).  $T_2$  is affected to a lesser extent than  $T_1$ . Eventually, when  $c_a^0$  exceeds a threshold,  $T_1$  becomes negative, i.e. the drug must be administered right away without a waiting period, i.e. the region of drug concentrations where the treatment starts right away increases with increasing pre-aging of the system.

**S3.6.2. Comparison between inhibition of primary or secondary nucleation depending on initial aggregate concentration.** We now use the optimal control calculated in the presence of an initial concentration, Eq. (S109), to understand how the pre-aging level of the patient impacts the decision to inhibit primary or secondary nucleation (see Sec. S3.4.6). To this end, we first estimate the total cost associated with the optimal inhibition of secondary nucleation, which reads

$$\text{Cost}_{2\text{nd}}[c_a, c_d] = \zeta c_d (T_2 - T_1) + \frac{\alpha_0}{\kappa_0^2} \left(1 + \frac{\kappa_0 c_a^0}{\alpha}\right) e^{\kappa_0 T} \cdot e^{-(\kappa_0 - \kappa)(T_2 - T_1)}. \quad [\text{S110}]$$

Using Eq. (S109), we find

$$\begin{aligned} \text{Cost}_{2\text{nd}}[c_a, c_d] = \zeta c_d \left[ \frac{\kappa_0 T}{\kappa_0 - \kappa_0} - \frac{1}{\kappa_0 - \kappa_0} \ln\left(\frac{\zeta \kappa_0^2 c_d}{\alpha_0(\kappa_0 - \kappa)\Gamma}\right) + \frac{2\kappa - \kappa_0}{\kappa_0(\kappa_0 - \kappa)} \ln\left(1 + \frac{\kappa_0 c_a^0}{\alpha_0}\right) \right] \\ + \frac{\alpha_0}{\kappa_0^2} \left(1 + \frac{\kappa_0 c_a^0}{\alpha}\right) \left[ \frac{\zeta \kappa_0^2 c_d}{\alpha(\kappa_0 - \kappa)} + \left(1 + \frac{\kappa_0 c_a^0}{\alpha}\right)^{\frac{\kappa_0 - 2\kappa}{\kappa_0}} \right]. \end{aligned} \quad [\text{S111}]$$

The total cost associated with inhibition of primary nucleation is similarly calculated as (see Eq. (S92)):

$$\text{Cost}_{1\text{st}}[c_a, c_d] \simeq \frac{\alpha_0 - \alpha}{\kappa_0^2} e^{\kappa_0(T - T_2)} + \frac{\alpha}{\kappa_0^2} \left(1 + \frac{\kappa_0 c_a^0}{\alpha}\right) e^{\kappa_0 T} + \zeta c_d T_2. \quad [\text{S112}]$$

The optimal cost for inhibition of primary nucleation is then

$$\text{Cost}_{1\text{st}}[c_a, c_d] \simeq \frac{\alpha}{\kappa_0^2} \left(1 + \frac{\kappa_0 c_a^0}{\alpha}\right) e^{\kappa_0 T} + \zeta c_d \left[ T + \frac{1}{\kappa_0} - \frac{1}{\kappa_0} \ln\left(\frac{\zeta \kappa_0 c_d}{\alpha_0 - \alpha}\right) \right] + \frac{\alpha_0 - \alpha}{\kappa_0^2}. \quad [\text{S113}]$$

Keeping the leading order terms in Eq. (S111) and Eq. (S113), the condition

$$\text{Cost}_{1\text{st}}[c_a, c_d] < \text{Cost}_{2\text{nd}}[c_a, c_d] \quad [\text{S114}]$$

becomes

$$\frac{\alpha}{\kappa_0^2} \left(1 + \frac{\kappa_0 c_a^0}{\alpha}\right) e^{\kappa_0 T} + \zeta c_d T < \frac{\zeta c_d \kappa_0 T}{\kappa_0 - \kappa}. \quad [\text{S115}]$$

Hence, inhibiting primary nucleation is to be preferred over the inhibition of secondary nucleation when:

$$\frac{e^{\kappa_0 T}}{\kappa_0 T} < \frac{\zeta c_d \kappa}{\kappa_0 - \kappa} \frac{\kappa_0}{\alpha \left(1 + \frac{\kappa_0 c_a^0}{\alpha}\right)} \simeq \frac{\zeta c_d \kappa}{\alpha \left(1 + \frac{\kappa_0 c_a^0}{\alpha}\right)}. \quad [\text{S116}]$$

We note that increasing  $c_a^0$  favours the choice of inhibiting secondary nucleation over primary nucleation. Increasing the initial level of aggregates  $c_a^0$  successively reduces the first no treatment phase in the optimal protocol for secondary nucleation (see Fig. 3b of main text).

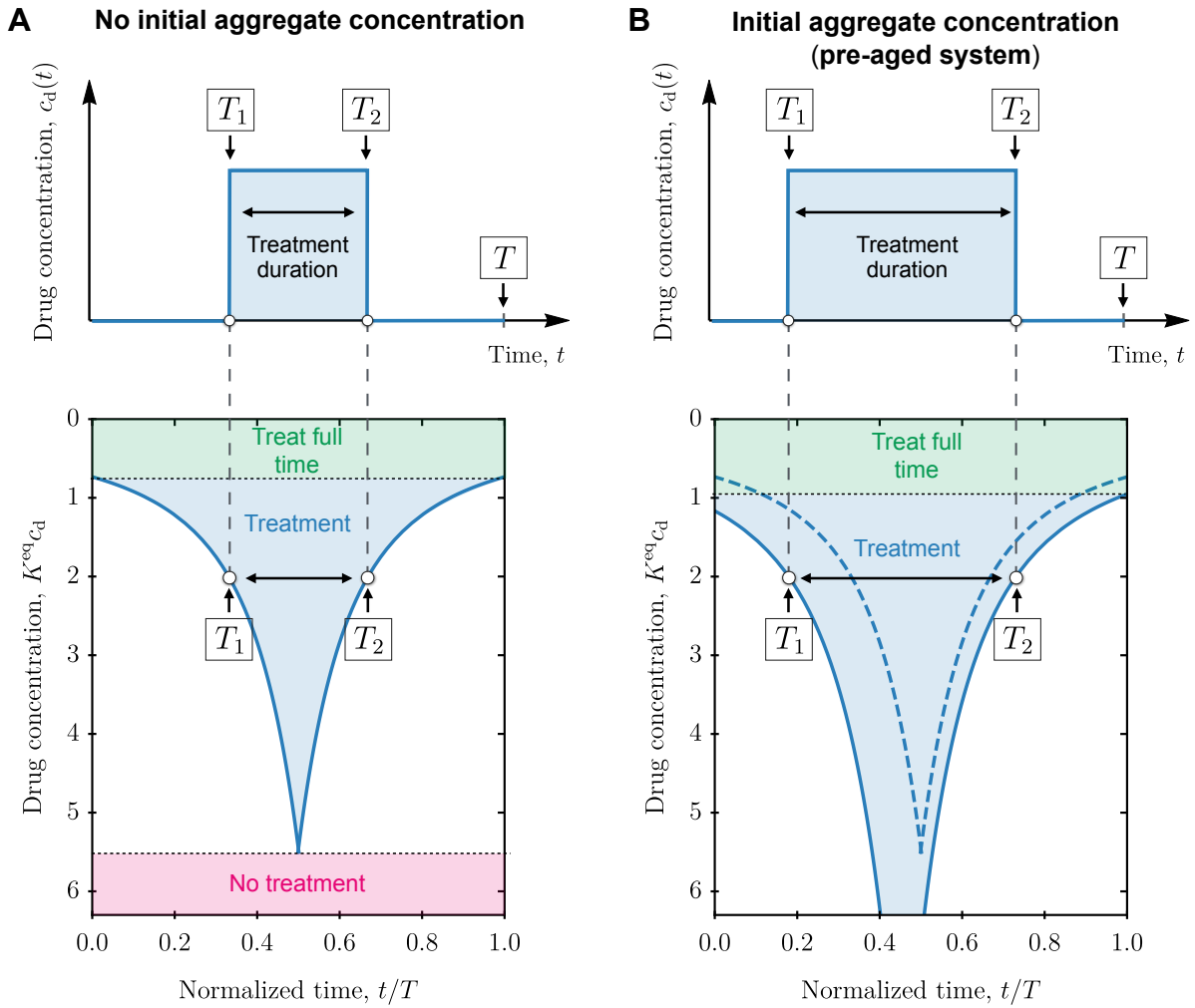


**Fig. S4.** Effect of initial aggregate concentration (pre-aged system) on optimal protocol for inhibition of secondary nucleation or growth. (a) Optimal protocol (start and end times) in the absence of initial concentration of aggregates. (b) Optimal protocol in the presence of an initial concentration of aggregates ( $\kappa_0 c_a^0 / \alpha_0 = 0.5$ ). Dashed lines are optimal switching times in the absence of an initial concentration of aggregates, for comparison. The parameters are the same as in Fig. 2b of the main text.

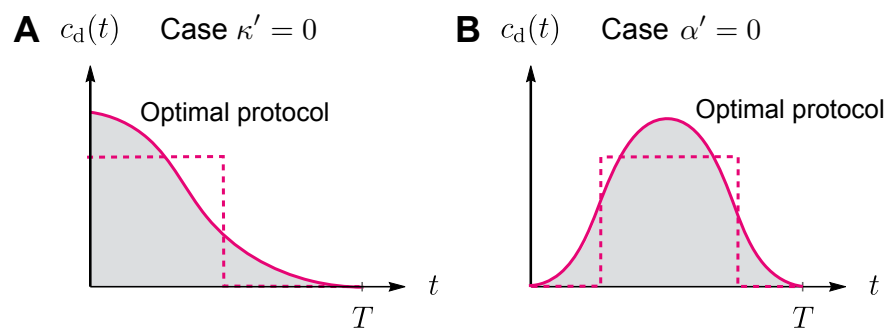


**Fig. S5.** Schematic representation of the optimal protocols for the inhibition of primary nucleation (a) and secondary nucleation or growth (b) for a non-linear cost function. The resulting optimal protocols are “smoothed-out versions” of the bang-bang controls that emerge in the linear case (dashed lines).

**S3.7. Optimal protocols emerging from non-linear cost functions.** In the main text, we have opted for a cost function that is linear in the drug and aggregate concentrations. This choice for the cost function resulted in optimal bang-bang controls and a key finding was that inhibition of primary nucleation requires early administration, while inhibition of secondary nucleation or growth requires late administration. We now show that this finding is robust in the sense that it remains valid also when the cost function is non-linear; the resulting optimal protocols are smoothed out versions of the bang bang control that emerges from the linear cost function. The function  $\mathcal{L}(c_d, c_a)$  can be expanded as Taylor series in the variables  $c_d$  and  $c_a$ . Hence, it is sufficient to focus on a cost function of the following form:

$$\text{Cost}[c_d, c_a] = \int_0^T dt \left( c_a(t)^m + \zeta c_d(t)^n \right), \quad [\text{S117}]$$

where  $m, n \geq 1$ . To solve the resulting optimal control problem, we apply again the variational recipe as introduced in section S3.1 and consider the Hamiltonian function, which is defined in Eq. (S55) and with a non-linear cost function Eq. (S117) reads:

$$\mathcal{H}[c_d(t), c_a(t), \lambda(t)] = c_a(t)^m + \zeta c_d(t)^n + \lambda(t) [\alpha(c_d(t)) + \kappa(c_d(t)) c_a(t)], \quad [\text{S118}]$$

The optimal control corresponds to a minimum of the Hamiltonian with respect to the drug concentration

$$\frac{\partial \mathcal{H}}{\partial c_d} = 0, \quad [\text{S119}]$$

which yields the following condition

$$\frac{\partial \mathcal{H}}{\partial c_d} = n\zeta c_d(t)^{n-1} + \lambda(t) [\alpha'(c_d(t)) + \kappa'(c_d(t)) c_a(t)] = 0. \quad [\text{S120}]$$

Let us now consider the situations when the drug affects  $\alpha$  or  $\kappa$  only separately.

- When the drug affects only primary nucleation, we have  $\kappa' = 0$ , and so the optimal protocol is obtained as solution to the following equation

$$\frac{c_d(t)^{n-1}}{|\alpha'(c_d(t))|} = \frac{\lambda(t)}{n\zeta}. \quad [\text{S121}]$$

The function  $\alpha(c_d)$  is a monotonically decreasing function of  $c_d$  without points of inflection. Hence, the expression on the left-hand side of Eq. (S121) is a monotonically increasing function  $g$  of drug concentration  $c_d$ , which can therefore be inverted to yield the optimal protocol:

$$c_d(t) = g^{-1} \left( \frac{\lambda(t)}{n\zeta} \right). \quad [\text{S122}]$$

Since  $g$  is a monotonically increasing function, also its inverse  $g^{-1}$  is monotonically increasing (follows directly from the inverse function theorem). The co-state variable  $\lambda(t)$  is a monotonically decreasing function of time with  $\lambda(t=T) = 0$ . Hence, from Eq. (S122) it follows also that the optimal protocol  $c_d(t)$  is a monotonically decreasing function of time, which is maximal when  $t = 0$  and equals zero when  $t = T$  (note that  $g(c_d = 0) = 0$ ; hence  $g^{-1}(0) = 0$ ). Thus, inhibition of primary nucleation always requires an early administration optimal protocol irrespective of the exponent  $n$  in the cost function (Fig. S5(a)).

- When the drug inhibits secondary nucleation or growth, i.e.  $\alpha' = 0$ , the optimal protocol is obtained by solving the following equation

$$\frac{c_d(t)^{n-1}}{|\kappa'(c_d(t))|} = \frac{\lambda(t)c_a(t)}{n\zeta}. \quad [\text{S123}]$$

Using similar arguments as for the inhibition of primary nucleation only, we introduce a function  $h(c_d) = c_d^{n-1}/|\kappa'(c_d)|$  and the optimal protocol emerges as

$$c_d(t) = h^{-1} \left( \frac{\lambda(t)c_a(t)}{n\zeta} \right). \quad [\text{S124}]$$

The concentration of aggregates satisfies  $c_a(t=0) = 0$ , while the co-state variable  $\lambda$  satisfies  $\lambda(t=T) = 0$ . Thus, the optimal protocol is a non-monotonic function of time, which is zero at the start  $t = 0$  and at the end  $t = T$  and has a maximum in between 0 and  $T$ . Thus, inhibition of secondary nucleation or elongation requires a late administration optimal protocol (Fig. S5(b)).

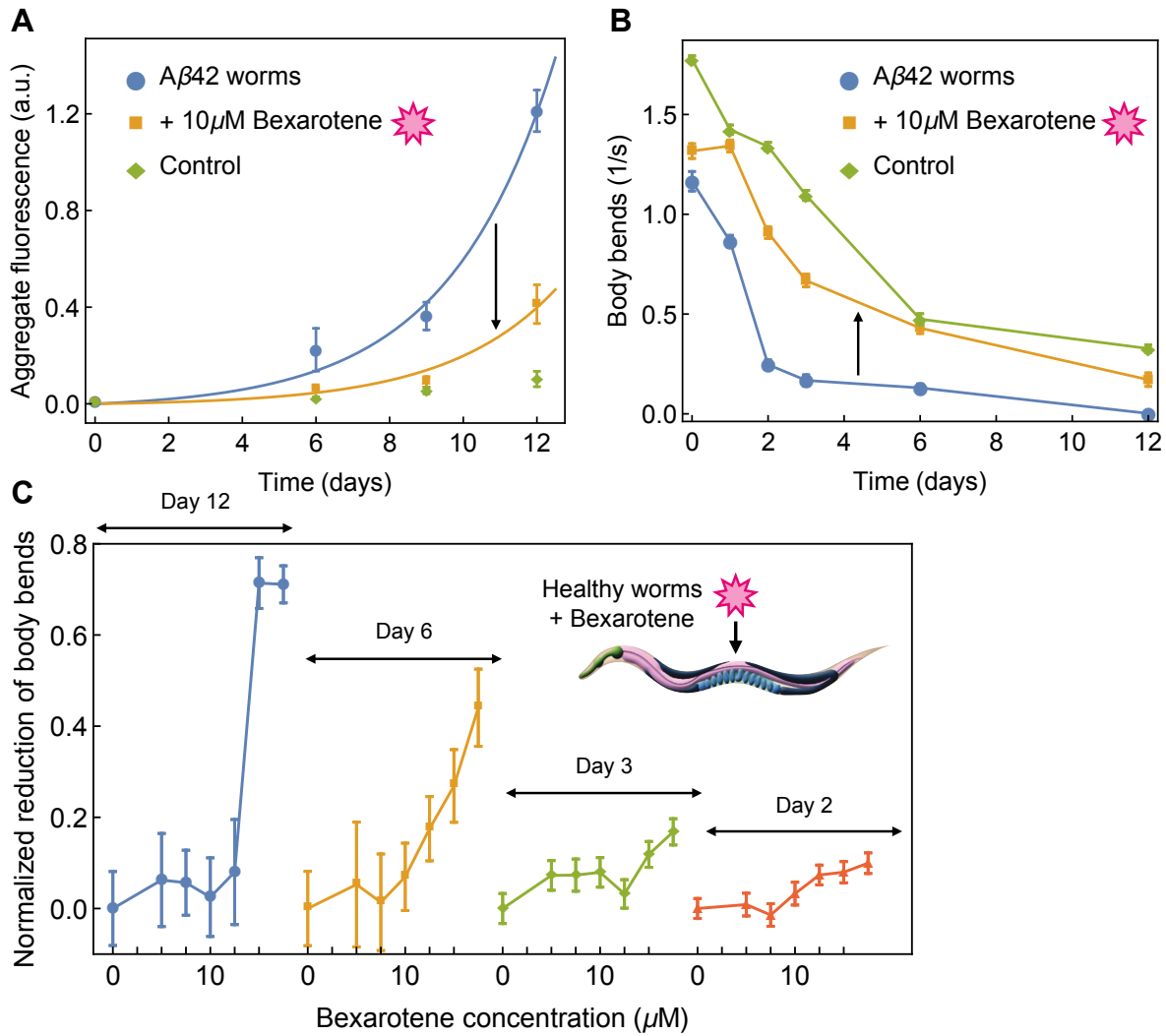


**Fig. S6.** (a) Aggregation of A $\beta$ 42 inside *C. elegans* worms as a function of time for A $\beta$ 42 worms (blue), A $\beta$ 42 worms treated with 10  $\mu$ M Bexarotene, administered 72 hours before adulthood (orange), and control worms (green). The aggregation data in untreated and treated A $\beta$ 42 worms are fitted to exponential increase,  $M_a(t) = \frac{\alpha_0}{2\beta_0} (e^{\kappa_0 t} - 1)$  (solid lines). The fit to untreated worms yields  $\kappa_0 \simeq 0.34 \text{ days}^{-1}$ ; the data for aggregation with Bexarotene are fitted by keeping  $\kappa_0$  fixed and varying  $\alpha_0$  (rate of primary nucleation) only. Thus, the action of Bexarotene on aggregation data in worms is consistent with inhibition of primary nucleation. (b) Frequency of body bends over time for A $\beta$ 42 worms (blue), A $\beta$ 42 worms treated with 10  $\mu$ M Bexarotene, administered 72 hours before adulthood (orange), and control worms (green). (c) Toxicity of Bexarotene in *C. elegans* worms. The data show normalized reduction in frequency of body bends (relative to healthy control worms) measured in healthy *C. elegans* worms treated with increasing concentration of Bexarotene. The reduction in frequency of body bends is shown at days  $T = 12, 6, 3,$  and  $2$  of adulthood. The toxic effects of Bexarotene increase with Bexarotene concentration and exposure time. This is consistent with our cost functional which increases with increasing drug concentrations and integration time  $T$ .



## References

1. T. P. J. Knowles *et al.* An analytical solution to the kinetics of breakable filament assembly. *Science* **326**, 1533 (2009).
2. S. I. A. Cohen *et al.* Nucleated polymerization with secondary pathways. I. Time evolution of the principal moments. *J. Chem. Phys.* **135**, 08B615 (2011).
3. T. C. T. Michaels and T. P. Knowles, Mean-field master equation formalism for biofilament growth. *Am. J. Phys.* **82**, 476 (2014).
4. T. C. T. Michaels, *et al.* Chemical kinetics for bridging molecular mechanisms and macroscopic measurements of amyloid fibril formation. *Annu. Rev. Phys. Chem.* **69**, 273 (2018).
5. P. Arosio *et al.* Kinetic analysis reveals the diversity of microscopic mechanisms through which molecular chaperones suppress amyloid formation. *Nature Comms* **7**, (2016).
6. T. C. T. Michaels *et al.* Hamiltonian dynamics of protein filament formation. *Phys. Rev. Lett.* **116**, 038101 (2016).
7. S. I. A. Cohen *et al.* Proliferation of amyloid- $\beta$ 42 aggregates occurs through a secondary nucleation mechanism. *Proc. Natl. Acad. Sci. USA* **110**, 9758 (2013).
8. C. N. Hinshelwood, On the chemical kinetics of autolytic systems. *J. Chem. Soc. (Resumed)* 745 (1952).
9. S. I. A. Cohen *et al.* A molecular chaperone breaks the catalytic cycle that generates toxic A $\beta$  oligomers. *Nature Struct. Mol. Biol.* **22**, 207 (2015).
10. J. Habchi *et al.* An anticancer drug suppresses the primary nucleation reaction that initiates the production of the toxic A $\beta$ 42 aggregates linked with Alzheimer's disease. *Sci. Adv.* **2**, e1501244 (2016).
11. J. Habchi *et al.* Systematic development of small molecules to inhibit specific microscopic steps of A $\beta$ 42 aggregation in Alzheimer's disease. *Proc. Natl. Acad. Sci. USA* **114**, E200 (2017).
12. F. A. Aprile *et al.* Inhibition of  $\alpha$ -Synuclein Fibril Elongation by Hsp70 Is Governed by a Kinetic Binding Competition between  $\alpha$ -Synuclein Species. *Biochemistry* **56**, 1177 (2017).
13. E. Monsellier and F. Chiti, Prevention of amyloid-like aggregation as a driving force of protein evolution. *EMBO reports* **8**, 737 (2007).
14. S. T. Ferreira, M. N. Vieira, and F. G. De Felice, Soluble protein oligomers as emerging toxins in Alzheimer's and other amyloid diseases. *IUBMB life* **59**, 332 (2007).
15. D. Eisenberg and M. Jucker, The amyloid state of proteins in human diseases. *Cell* **148**, 1188 (2012).
16. C. M. Dobson, The Amyloid Phenomenon and Its Links with Human Disease. *Cold Spring Harbor Persp. Biol.* **9**, a023648 (2017).
17. C. M. Bender and S. A. Orszag, *Advanced mathematical methods for scientists and engineers I: Asymptotic methods and perturbation theory* (Springer, 2013).
18. J. K. Nicholson, J. Connelly, J. C. Lindon, and E. Holmes, Metabonomics: a platform for studying drug toxicity and gene function. *Nature Rev. Drug Discov.* **1**, 153 (2002).
19. L. M. Hocking, *Optimal control: an introduction to the theory with applications* (Oxford University Press, 1991).